Friction
https://doi.org/10.1007/s40544-023-0817-8
ISSN 2223-7690
CN 10-1237/TH
REVIEW ARTICLE

Biomechanical energy harvesting technologies for wearable electronics: Theories and devices

Xiaowen LI, Xu ZENG, Junwei LI, Boyuan LI, Yu CHEN, Xiaosheng ZHANG*
University of Electronic Science and Technology of China, Chengdu 611731, China
Received: 23 April 2023 / Revised: 19 June 2023 / Accepted: 23 August 2023

Abstract: Wearable biomechanical energy harvesting devices have received a lot of attention recently, benefiting from the rapid advancement of theories and devices in the field of the micro electromechanical system (MEMS). They not only fulfil the requirements for powering wearable electronic devices but also provide an attractive prospect for powering self-powered flexible electronic devices when wearing. In this article, we provide a review of the theories and devices of biomechanical energy harvesting technology for wearable applications. Three different forms of biomechanical energy harvesting mechanisms, including the piezoelectric effect, electromagnetic effect, and electrostatic effect, are investigated in detail. The fundamental principle of converting other types of energy from the biomechanical environment into electrical energy, as well as the most commonly-used analytical theoretical models, are outlined for each process. Therefore, the features, properties, and applications of energy harvesting devices are summarized. In addition, the coupled multi-effect hybrid energy harvesting devices are listed, showing the various possibilities of biomechanical energy harvesting devices for serving as sources, sensors, and actuators. Finally, we present perspectives on the future trends of biomechanical energy harvesting devices for wearable electronics applications.

Keywords: micro electromechanical system (MEMS); nanogenerators; biomechanical energy harvesters; wearable electronics

1 Introduction

In recent years, with the continuous expansion of the application of wearable electronic devices, micro-nano energy harvesting devices have made great progress [1–5]. They have become an indispensable part of our lives, integrated into sports [6–8], medical treatment [9–11], communication [12, 13], and entertainment [14, 15]. Among them, biomechanical energy harvesting devices collect energy from the living environment, especially from the human body. They have the advantage of being lightweight, showing the possibility of realizing highly efficient self-powered devices [16–18]. In addition, higher output energy density and higher efficiency have always been the goals pursued by researchers. Although theories related to biomechanical energy harvesting devices are relatively mature, it has become very difficult to make devices with better performance. At present, for biomechanical energy harvesting, the problems of flexibility, miniaturization, integration, and biocompatibility still need to be solved.

Energy harvesting refers to the conversion of other forms of energy into electrical energy, such as photovoltaic effect [19, 20], thermoelectric effect [21, 22], piezoelectric effect [23, 24], electromagnetic effect [25, 26], and electrostatic effect [27–29]. These technologies have their own principles, and devices based on these energy harvesting technologies have unique characteristics and applicable conditions. For example, the direct current (DC) output of photovoltaic generators (PVG) is continuous and the output power

* Corresponding author: Xiaosheng ZHANG, E-mail: zhangxs@uestc.edu.cn

is high, which is suitable for large-scale industrial arrays. Their high energy conversion efficiency has huge advantages for regions with high light intensity throughout the year, but they are not conducive to integration into small electronic devices. Since wearable applications for human motions requires accessing sustainable energy but PVG is limited by sustainable sunlight, especially applying indoors. Thermoelectric generators (TEG) work according to the temperature difference with good power generation continuity and reliability, but the output power and the energy conversion efficiency are low, which is not suitable for high-performance device applications. Moreover, thermoelectrics requires significant temperature gradients for efficient operation but this is a difficult environmental constraint for wearable applications on the human body. Piezoelectric nanogenerators (PENGs) are very sensitive to tiny deformations due to the piezoelectric effect based on the crystal structure and are easy to integrate and miniaturize on the micro/nanoscale, but their energy conversion efficiency and output power are low. The advantage of the electromagnetic generator (EMG) is that it has high energy conversion efficiency with a large current output, but the voltage output is generally relatively low. It is worth mentioning that it is very difficult to miniaturize due to the need for coils and bulky magnets. In addition, triboelectric nanogenerators (TENGs) have sustainable, high-output properties due to the triboelectric effect of materials. Because of its simple structure, it is easy to integrate and miniaturize with flexibility, and has obtained great success in the field of wearable electronics. But at the same time, its problems are concentrated on the pulse and unstable output, which means it needs an additional rectifier module to realize DC output.

The harvested biomechanical energy mainly comes from human motions (e.g., limb bending, walking, running, pressing, and heartbeat). Since piezoelectric, electromagnetic, and electrostatic mechanical energy harvesting technologies have their own characteristics, they are all suitable for wearable applications. Theories and devices based on these three techniques and the hybrid devices with coupled multi-effect are the focus of this review. For each effect, we summarize the existing theories, analyze the basic principles and theoretical models, and give some key formulas. In addition, we also list the existing devices based on these three technologies, and summarize the structure, materials, and properties of the devices. Finally, hybrid generator devices with coupled multi-effect are also summarized. This kind of hybrid generator device has only been studied in recent years and has more advantages than single-type generators, such as a significant increase in power generation efficiency. In the future, in wearable applications, the theories of biomechanical energy harvesting will be more complete, and the performance of the devices will be better. Their self-powering, sensing, and actuation capabilities offer promising feasibility for building smart wearable microsystems.

The schematic diagram of the technical route of this review is shown in Fig. 1. This review highlights the following four points: <i> Studies of biomechanical energy harvesting are summarized, which can be divided into piezoelectric effect, electromagnetic effect, and electrostatic effect; <ii> the theoretical models of biomechanical energy harvesters are studied, including some key formulas, and their applicable conditions; <iii> devices for wearable electronic applications of biomechanical energy harvesting are summarized; and <iv> characteristics of multi-effect coupled hybrid energy harvesting devices are summarized and the prospect of building a new generation of wearable systems is proposed.

2 Theories and devices for biomechanical energy harvesting

In this section, three types of biomechanical energy harvesting mechanisms are emphasized, i.e., piezoelectric energy harvesting mode, electromagnetic energy harvesting mode, and electrostatic energy harvesting mode. For each type, the working principles and theories of biomechanical energy harvesters are studied in detail. Finally, coupled multi-effect composite energy harvesting mechanism is studied, and the application of biomechanical energy harvesting devices in the wearable field is discussed.

2.1 Piezoelectric energy harvesting

The piezoelectric effect was first discovered by the French physicists Jacques and Pierre Curie brothers

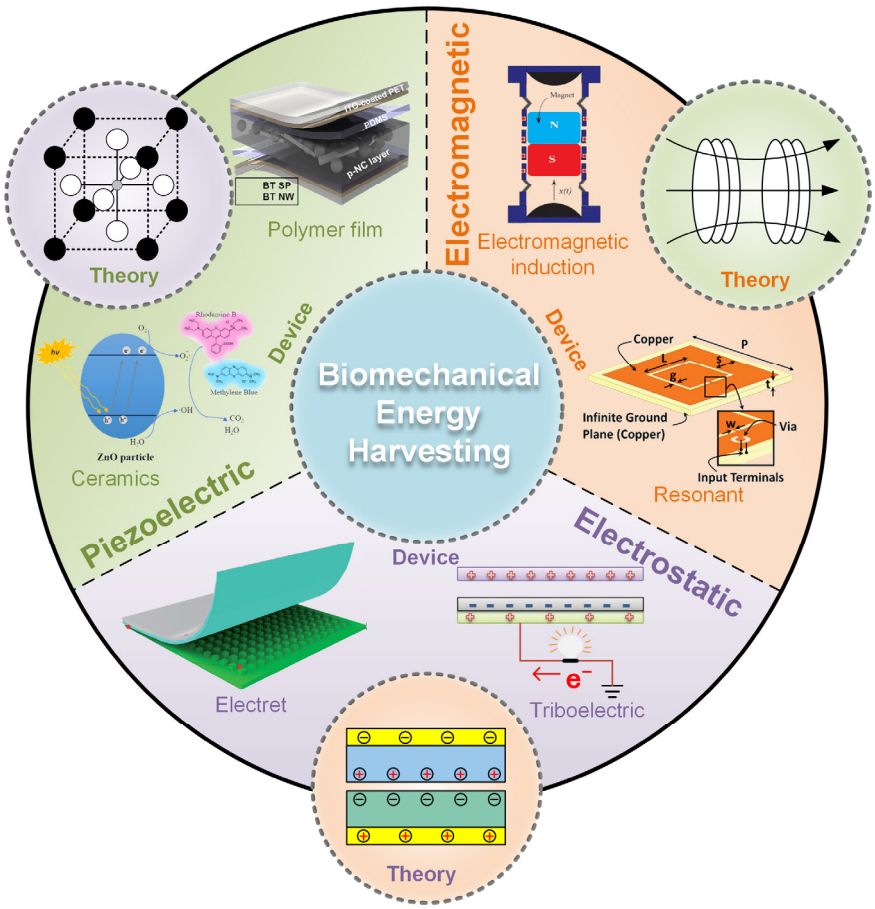

Fig. 1 Overview of the progress of biomechanical energy harvesting for wearable electronic applications, including piezoelectric effect, electromagnetic effect, and electrostatic effect. In the piezoelectric effect, the devices (e.g., ceramics, polymer film) are summarized [30, 31]. Reproduced with permission from Ref. [30], © Elsevier, 2019; Reproduced with permission from Ref. [31], © Elsevier, 2017. And the theory is summarized [32]. In the electromagnetic effect, the devices (e.g., resonant, electromagnetic induction) are summarized [33]. Reproduced with permission from Refs. [33, 34], © AIP, 2015; Reproduced with permission from Ref. [34], © Elsevier, 2018. And the theory is summarized [35]. In the electrostatic effect, the devices (e.g., electret, triboelectric) are summarized [36, 37]. Reproduced with permission from Ref. [36], © Royal Society of Chemistry, 2018; Reproduced with permission from Ref. [37], © Wiley, 2017. And the theory is summarized [38].

in 1880. Certain materials, e.g., ceramics, crystals, and polymers, will generate electrical polarization in response to applied mechanical stress, driving polarization charges across the two sides of the crystal, creating a potential difference. This conversion of mechanical energy into electrical energy is known as the piezoelectric effect. Similarly, the crystal also exhibits the opposite effect. When an electric field is applied, it will produce mechanical strain or deformation, i.e., the reverse piezoelectric effect.

2.1.1 *Principles of piezoelectric theory*

Figure 2 presents piezoelectric schematic diagrams and theories (see Note 1 in the Electronic Supplementary Material (ESM) for the piezoelectric theories in details) to explain more details about the mechanisms. For the crystal with a structure of the planar hexagonal cell (Fig. 2(a)<i>), the initial polarization is zero [39]. If the stress along the y-direction is applied (Fig. 2(a)<ii>), the equivalent center of the positive charges will no longer coincide with that of the negative charges, which will change the electric dipole moment and form the polarization in the y-direction. Similarly, since the crystal is symmetric about y, the stress in the x-direction will also only create a net polarization in the y-direction (Fig. 2(a)<iii>). Therefore, based on the microstructural changes of crystals, there are three types of piezoelectric

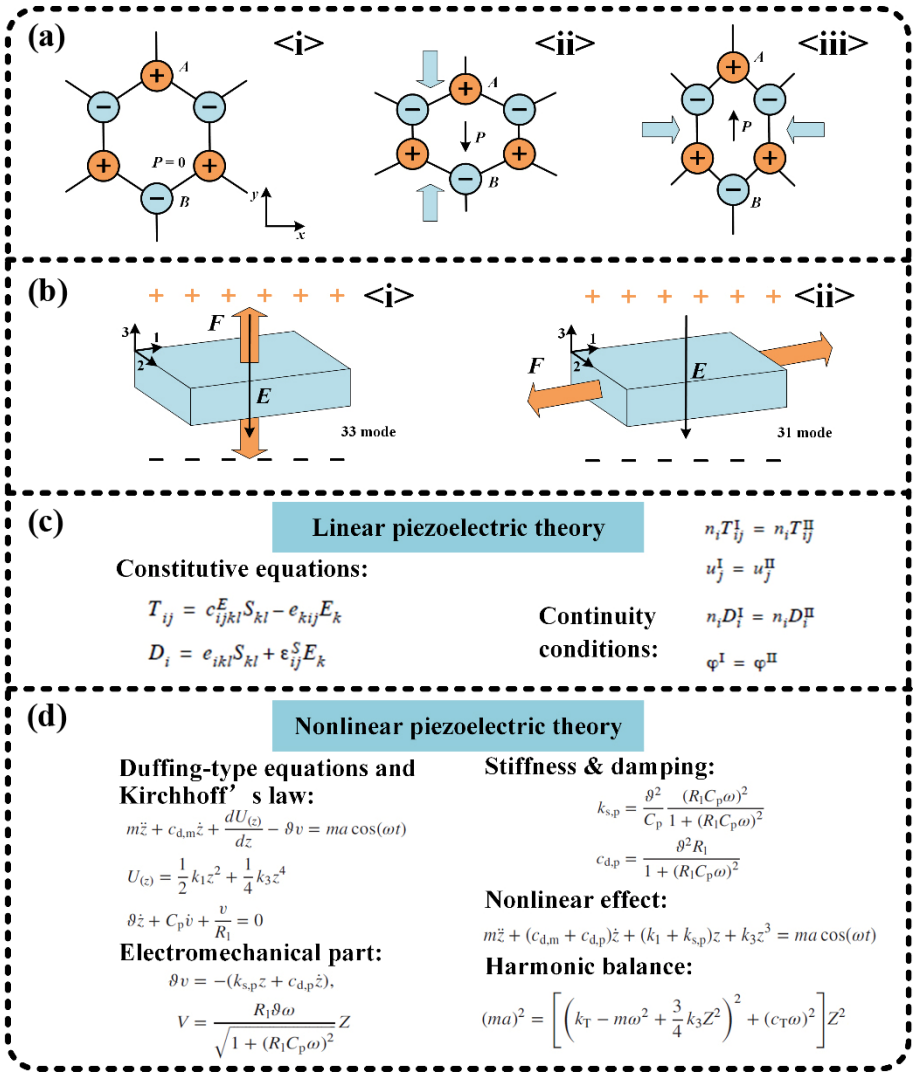

Fig. 2 Piezoelectric theories for biomechanical energy harvesting. (a, b) Explanation of piezoelectric mechanism and schematic diagram of working mode. (a) Piezoelectric mechanism in a hexagonal unit cell with no symmetry center, including <i> no stress, <ii> stress in *y*-direction, and <iii> stress in *x*-direction [39]. (b) Vibration modes including <i> d_{33} (transverse mode) and <ii> d_{31} (longitudinal mode) for piezoelectric energy harvesting [40]. (c, d) Theories for linear and nonlinear piezoelectric effects. (c) Linear theory of piezoelectricity [42]. (d) Nonlinear theory of piezoelectricity [43].

energy harvesting, d_{33} mode, d_{11} mode, and their hybrids [40]. When the polarization is parallel to the stress direction, it is recorded as the transverse mode, i.e., d_{33} mode (Fig. 2(b)<i>). Similarly, when the polarization is perpendicular to the stress direction, it is recorded as the longitudinal mode, i.e., d_{31} mode (Fig. 2(b)<ii>).

Linear piezoelectricity is the most widespread technology and has been widely used in many fields, e.g., biomechanical energy harvesting [41]. In general, from the energy conservation in a linear piezoelectric continuum, the first law of thermodynamics can be derived. Based on these theories, the linear piezoelectric constitutive equations will be satisfied as Eqs. (1) and (2), as shown in Fig. 2(c) [42]:

$$T_{ij} = c^E_{ijkl}S_{kl} - e_{kij}E_k \quad (1)$$

$$D_i = e_{ikl}S_{kl} + \varepsilon^S_{ij}E_k \quad (2)$$

where S and T are strain and stress tensors, respectively; E and D are the electric field and electric displacement, respectively.

Here, Eq. (2) describes the piezoelectric effect, i.e, the conversion of mechanical energy to electrical energy.

Conversely, Eq. (1) shows how electrical energy is converted into mechanical deformation according to the reverse piezoelectric effect. If there is a discontinuous material surface, the boundary conditions can be derived from differential equations to satisfy the continuity condition, as shown in Fig. 2(c).

Since the linear piezoelectricity is limited by the excitation frequency, it has the characteristic of narrow bandwidth. Therefore, nonlinear theories have also been developed to overcome the disadvantages, as shown in Fig. 2(d). The nonlinear dynamic equations are based on Duffing-type equations and Kirchhoff's law [43]:

$$m\ddot{z} + c_{\mathrm{d,m}}\dot{z} + \frac{\mathrm{d}U(z)}{\mathrm{d}z} - \vartheta v = ma\cos(\omega t) \tag{3}$$

$$U(z) = \frac{1}{2}k_1 z^2 + \frac{1}{4}k_3 z^4 \tag{4}$$

$$\vartheta\dot{z} + C_{\mathrm{p}}\dot{v} + \frac{v}{R_1} = 0 \tag{5}$$

where m and $c_{\mathrm{d,m}}$ are effective mass and mechanical damping factor, respectively; z and v are the displacement of the mass and the voltage across the load R_1, respectively; k_1 and k_3 refer to linear and nonlinear restoring, respectively; C_{P} and ϑ are the equivalent piezoelectric material capacitance and the electromechanical coupling coefficient, respectively; $U(z)$ is the mechanical potential energy of the vibrating system; a and ω are the acceleration amplitude and the angular frequency, respectively.

The electromechanical part is modeled by the piezoelectric electromechanical parameter ϑ. And then, the stiffness and damping for the piezoelectric effect are depicted in Fig. 2(d). Therefore, the nonlinear piezoelectric effect is obtained according to the above analysis.

2.1.2 *Piezoelectric devices*

Piezoelectric devices are of great significance in biomechanical energy harvesting field due to their simple structure and ease of use. As shown in Fig. 3, piezoelectric devices are generally divided into two categories according to the materials, namely piezoelectric ceramics (Figs. 3(a)–3(d)) and piezoelectric polymers (Figs. 3(e)–3(h)). Here, piezoelectric ceramics are usually very brittle and have poor flexibility, but they have a large electromechanical coupling constant and a high energy conversion rate, which can make the fabricated piezoelectric devices perform better. In contrast, piezoelectric polymers have excellent flexibility, but they suffer from low electromechanical coupling constants and low energy conversion rates compared to ceramics.

The early piezoelectric ceramic devices used ceramics directly, which had poor flexibility. Recent studies tended to make ceramics into nanowires. Figure 3(a) reports a nanogenerator based on $BaTiO_3$ nanowires-polyvinyl chloride (PVC) composite single fiber [44]. Firstly, the researchers fabricated <001> oriented $BaTiO_3$ nanowires using topochemical synthesis. Secondly, $BaTiO_3$ nanowires were implanted into PVC matrix by spinning method to form composite fibers. Finally, the composite fibers and the receiving substrate covered with the ink-printed interdigital electrodes constitute a nanogenerator. When the finger is bent, the wearable nanogenerator exhibits an output voltage of 0.9 V and an output current of 10.5 nA. This study demonstrates the prospect of piezoelectric ceramic-based composite fibers in piezoelectric biomechanical energy harvesting devices. In addition, there are also studies focusing on nanowires [45]. The study in Fig. 3(b) successfully synthesized InN nanowires (NWs) by the vapor-liquid-solid (V-L-S) process. When the direction of the transverse force applied to the InN NW changes, its piezoelectric potential can be positive, negative or zero. For the output voltage of the nanogenerator, approximately 40% to 55% of them are in the range of −1 and −20 mV, 25% to 30% will exceed −100 mV and some output voltages reach the level of −1,000 mV. In this study, the Schottky barrier formed between the electrode and the NW plays a crucial role in the energy harvesting process. It not only acts as a rectifier to determine the direction of carrier flow but also affects the efficiency and performance of piezoelectric nanogenerators. To minimize the limitation that piezoelectric ceramics are too hard, a large-area nanocomposite generator device based on lead zirconate titanate (PZT) nanoparticles is proposed [46]. PZT-based piezoelectric devices have been widely used in commercial fields, including energy

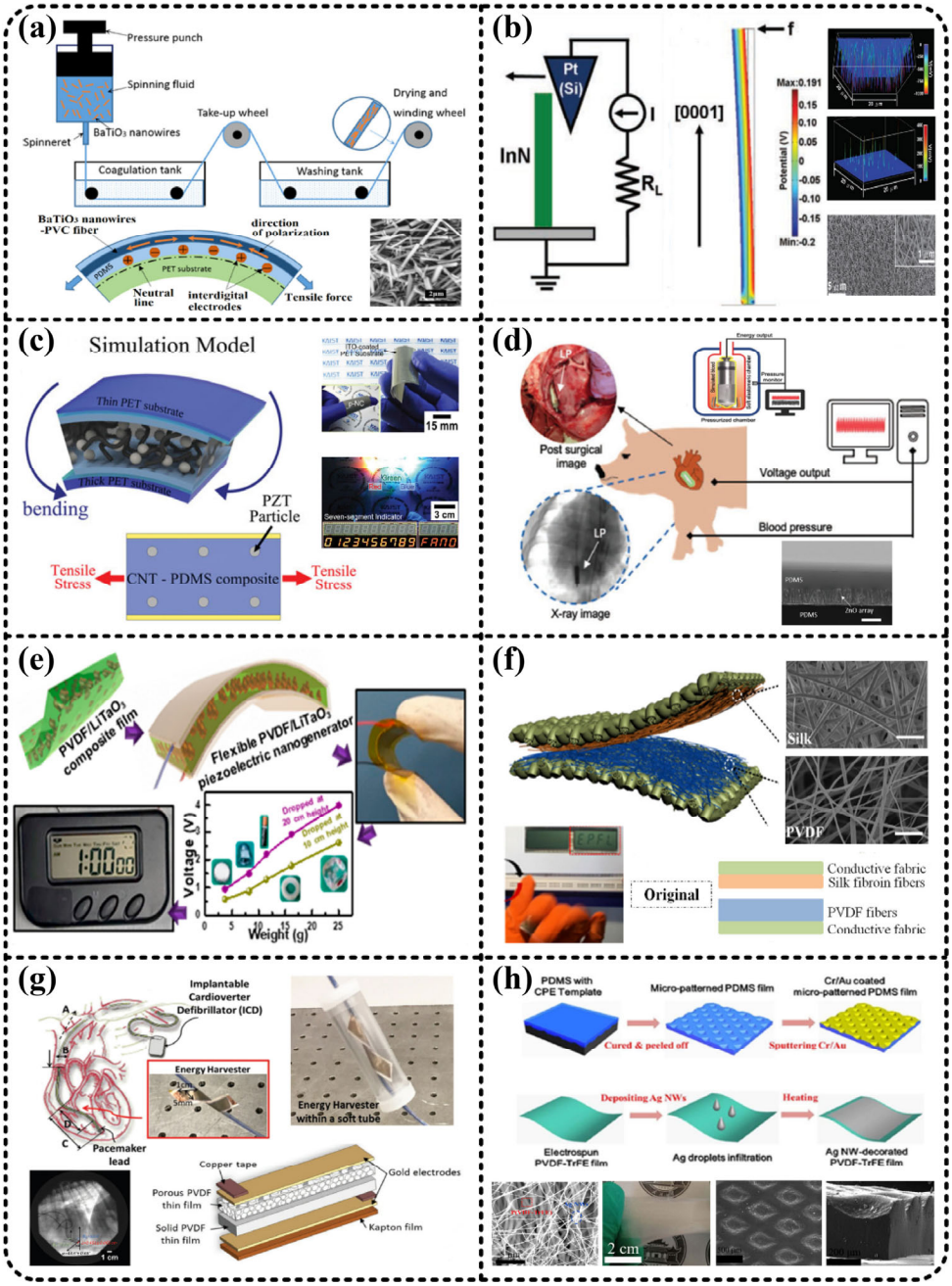

Fig. 3 Piezoelectric devices used for biomechanical energy harvesting. (a–d) Energy harvesting devices made of piezoelectric ceramic materials. (a) A nanogenerator based on $BaTiO_3$ nanowires-polyvinyl chloride (PVC) composite single fiber [44]. Reproduced with permission from Ref. [44], © Elsevier, 2015. (b) Single-InN-nanowire nanogenerator [45]. Reproduced with permission from Ref. [45], © Wiley, 2010. (c) A high-output large-area lead zirconate titanate (PZT)-based nanocomposite generator device [46]. Reproduced with permission from Ref. [46], © Wiley, 2013. (d) A highly flexible, stretchable, and biocompatible piezoelectric energy harvester by embedding ZnO nanoarrays in a polydimethylsiloxane (PDMS) [47]. Reproduced with permission from Ref. [47], © Wiley, 2021. (e–h) Energy harvesting devices made of piezoelectric polymer films. (e) Flexible piezoelectric nanogenerator (FPNG) based on piezoelectric film with $LiTaO_3$ nanoparticles loaded into poly(vinylidene difluoride) (PVDF) [48]. Reproduced with permission from Ref. [48], © ACS, 2021. (f) An all-fiber piezoelectrically enhanced generator device [49]. Reproduced with permission from Ref. [49], © Elsevier, 2018. (g) Flexible porous piezoelectric cantilever on a pacemaker lead based on polyvinylidene fluoride-trifluoroethylene (PVDF-TrFE) thin film [50]. Reproduced with permission from Ref. [50], © Wiley, 2019. (h) A piezoelectric nanogenerator with a polydimethylsiloxane (PDMS)/silver nanowire (Ag NW)/poly(vinylidene fluoride-trifluoroethylene) sandwich structure [51]. Reproduced with permission from Ref. [51], © AIP, 2015.

harvesting devices. As shown in Fig. 3(c), the device utilizes PZT particles to convert mechanical stress into electrical potential. In general, PZT ceramics with perovskite structures have tetragonal and rhombohedral symmetries below the Curie temperature (*Tc*). By applying an electric field near *Tc* to the ceramic, the dipole moment aligns with the direction of the external field, thus, a piezoelectric potential is created between the top and bottom electrodes. To overcome the non-stretchable disadvantage of ZnO, researchers fabricated a substrate-free biomechanical energy harvester of ZnO nanoarrays [47]. As shown in Fig. 3(d), the energy harvester fully embeds ZnO in silk-like polydimethylsiloxane (PDMS) elastomeric matrix for mechanical matching with human skin. The elastic modulus of the flexible device reaches 3.3 MPa and can be stretched up to 250% of its normal length. Further, the device harvests energy from hand finger movements and heartbeats through ex and in vivo tests. A device mounted on a leadless pacemaker in a porcine model produces an open circuit voltage of ≈ 0.3 Vpp.

In contrast, piezoelectric thin-film biomechanical energy harvesting devices have the flexibility and have been widely used. Some researchers used a ferroelectric material, i.e., lithium tantalite ($LiTaO_3$) nanoparticles to make a poly(vinylidene fluoride) (PVDF) piezoelectric composite film, and then combined aluminum electrodes on both sides to make a flexible piezoelectric nanogenerator (FPNG) [48]. Among them, the concentration of $LiTaO_3$ in PVDF has a significant effect on the electrical properties of FPNG. When the concentration was 2.5 wt%, the open-circuit voltage, short-circuit current, and power density values were ~18 V, ~1.2 μA, and ~25 mW/m^2, respectively. In this study (Fig. 3(e)), piezoelectric devices were used as weight sensors to harvest biomechanical energy. This energy was finally used to power LEDs or stored in capacitors to power other portable electronic devices. In Ref. [49], the researchers propose an all-fiber piezoelectrically enhanced generator. This device was formed from silk fibroin and polyvinylidene fluoride (PVDF) nanofibers and was fabricated by electrospinning. As shown in Fig. 3(f), the device is integrated into a conductive fabric to generate electricity through the deformation of PVDF fiber and the triboelectric of silk fibroin. Among them, the large specific surface area of the nanofibers endows the extraordinary ability of electrons, which enables the device to achieve a power density of 310 μW/cm^2. This device has a flexible appearance and good breathability and is easily embedded in any flexible fabric such as clothing. Additionally, the device can recognize various gestures and body movements. Further, the device is also suitable for use in a wearable fall alarm microsystem for elderly people or those working in high-risk areas. In addition, a unique design has been proposed for a typical biomechanical application, i.e., pacemaker leads [50]. As shown in Fig. 3(g), the new design employs a flexible porous PVDF-trifluoroethylene (TrFE) film within a dual-cantilever and extends the two free ends to harvest the energy of the heart. The maximum electrical output is 0.5 V and 43 nA at 1 Hz. It is noted that adding a mass of 31.6 mg to the cantilever resulted in 1.82 times more power than before. Further, by connecting two units in parallel, the simultaneous vibration can promote the conversion of energy, which provides a feasible solution for a practical pacemaker lead device. The study in Ref. [51] proposed a piezoelectric nanogenerator with a polydimethylsiloxane (PDMS)/ silver nanowire (Ag NW)/poly(vinylidene fluoride-trifluoroethylene) (P(VDF-TrFE)) sandwich structure (Fig. 3(h)). Here, Ag NWs facilitate the collection of charges generated by piezoelectric films, while micro-patterned PDMS films increase the sensitivity under external compression. The nanogenerator exhibits excellent performance with peak open-circuit voltage and short-circuit current of 1.2 V and 82 nA, respectively. In general, the nanofibers obtained by conventional electrospinning will wrinkle in the air environment, which reduces the energy conversion efficiency. Also, their compression works at low frequencies, resulting in not enough deformation for nanofibers to generate electricity. Therefore, the sensitivity brought by the introduction of PDMS greatly facilitates the realization of high-performance piezoelectric devices.

2.2 Electromagnetic energy harvesting

In 1831, Michael Faraday and Joseph Henry independently discovered the phenomenon of

electromagnetic induction. If the loop with conductors is placed in a magnetic field, a current will be induced as the magnetic flux passing through the loop varies with time. The changes in magnetic flux are closely related to mechanical motion, thus, electromagnetic generators can convert mechanical energy into electrical energy.

2.2.1 *Principles of electromagnetic theory*

Figure 4 presents electromagnetic schematic diagrams and theories (see Note 2 in the ESM for the electromagnetic theories in details) to explain more details about the mechanisms. For electromagnetic biomechanical energy harvesting devices, the theory of electromagnetic energy harvesting is mainly divided

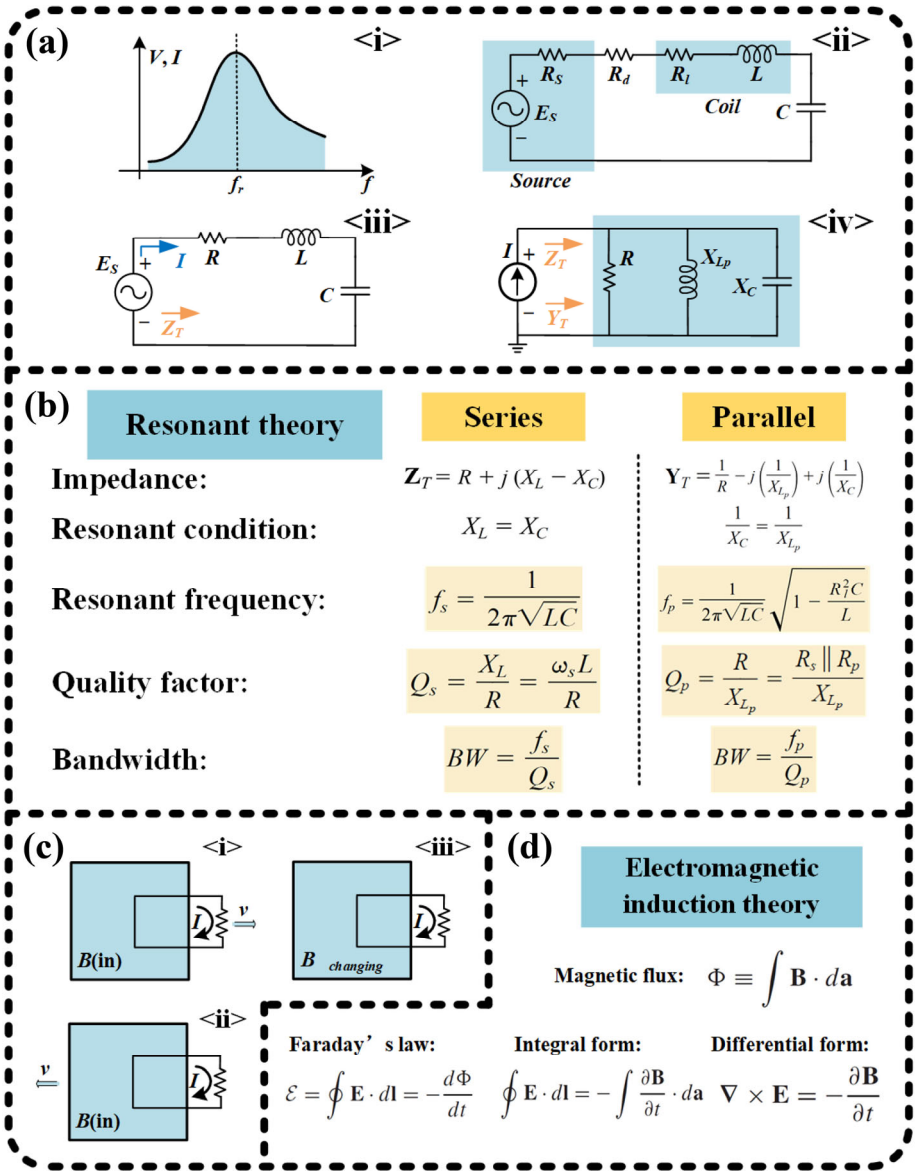

Fig. 4 Electromagnetic theories for biomechanical energy harvesting. (a, b) Explanation of the resonant circuits and schematic diagram [52]. (a) Resonant circuits in electrical and electronic systems, including <i> frequency response characteristic, <ii> basic configuration of a series resonant circuit, <iii> simplified form of the *RLC* series resonant circuit, and <iv> simplified form of the *RLC* parallel resonant circuit. (b) Theories of the series and parallel resonant circuits for electromagnetic energy harvesting. (c, d) Explanation of the electromagnetic induction and schematic diagram [53]. (c) Electromagnetic induction phenomenon, including conditions of <i> coil moving rightward, <ii> magnet moving leftward, and <iii> changing magnetic field of electromagnet. (d) Theory of electromagnetic induction for electromagnetic energy harvesting.

into two forms: resonance [52] and electromagnetic induction (i.e., cutting magnetic flux density lines) [53].

A resonant circuit is a combination of *R*, *L*, and *C* components and is the basis for the operation of electrical and electronic systems [52]. Its frequency response characteristic is shown in Fig. 4(a)<i>, with a response close to the maximum value at a certain frequency f_r, and a very low response at other frequencies. A resonant circuit must have both inductance and capacitance, and when a resonant state is reached, energy oscillates between reactive elements.

According to the connection form, resonant circuits are divided into series and parallel resonant circuits. For series resonant circuits, the resistance is unavoidable because of the internal resistance (R_s) of the source, the Joule losses (R_l) of the inductor, and the additional adjustment resistance (R_d). In general, the basic configuration of a series resonant circuit is shown in Fig. 4(a)<ii>. By combining the resistor elements in series into one equivalent resistance *R*, a simplified form of the *RLC* series resonant circuit of Fig. 4(a)<iii> is obtained. Here, equivalent resistance *R* satisfies the equations in Fig. 4(b).

The total input impedance of this circuit at any frequency is determined by

$$Z_T = R + j\left(X_L - X_C\right) \tag{6}$$

The series resonance will occur when the resonant condition is satisfied, i.e., the imaginary part of the impedance is zero. Thus, the resonant frequency is obtained (Fig. 4(b)):

$$f_s = \frac{1}{2\pi\sqrt{LC}} \tag{7}$$

Further, the expression of the quality factor *Q* will be derived. It describes the ratio of the reactive power of either the inductor or the capacitor to the average power of the resistor at resonance. And then, the 3-dB bandwidth is defined in Fig. 4(b).

In general, a simplified form of the *RLC* parallel resonant circuit is shown in Fig. 4(a)<iv>. Similar to the series resonant circuits, for parallel resonant circuits, the equivalent resistance is the parallel of source internal resistance (R_s) and the parallel resistance (R_p). The total input admittance of this circuit and the resonant frequency are shown in Eqs. (8) and (9), respectively.

$$Y_T = \frac{1}{R} - j\left(\frac{1}{X_{L_p}}\right) + j\left(\frac{1}{X_C}\right) \tag{8}$$

$$f_p = \frac{1}{2\pi\sqrt{LC}}\sqrt{1-\frac{R_l^2 C}{L}} \tag{9}$$

And then, the quality factor *Q* and the 3-dB bandwidth are shown in Fig. 4(b).

Another form of electromagnetic energy harvesting is electromagnetic induction, i.e., cutting magnetic flux density lines [53]. As shown in Fig. 4(c)<i>, a flowing current occurs when the loop of wire coil with a magnetic flux density passing through is pulled to the right. Since the motion is relative, if the magnet that generates the magnetic flux density is pulled to the left and the coil remains stationary, an induced current will also be generated in the coil, as shown in Fig. 4(c)<ii>. Both Figs. 4(c)<i> and 4(c)<ii> correspond to the motional electromotive force, which are one of the most widely used theories in biomechanical energy harvesting devices. In Fig. 4(c)<iii>, when the coil and the electromagnet remain stationary, adjusting the current in the electromagnet changes the magnetic flux density, which also induces a current in the coil. And this is the case of induced electromotive force. The reason for all cases can be summed up as that a changing magnetic field induces an electric field.

As shown in Fig. 4(d), magnetic flux is defined as the area integral of the magnetic flux density over the cross-section *a*. On one hand, the integral of the electric field along the closed-loop is the electric potential. On the other hand, Faraday's law is expressed as a time-varying magnetic flux that forms an induced electromotive force:

$$\varepsilon = \oint \boldsymbol{E}\cdot \mathrm{d}\boldsymbol{l} = -\frac{\mathrm{d}\Phi}{\mathrm{d}t} \tag{10}$$

According to the above analysis, the integral form of Faraday's law is derived in Fig. 4(d). Applying the identity of Stokes' theorem on the integral form of Faraday's law, the differential form is expressed as

$$\nabla \times \boldsymbol{E} = -\frac{\partial \boldsymbol{B}}{\partial t} \tag{11}$$

2.2.2 Electromagnetic devices

Electromagnetic devices have been widely used in the biomechanical energy harvesting field due to their high efficiency and long history of development [54, 55]. As shown in Fig. 5, electromagnetic devices are generally divided into two categories according to the working modes, namely resonant generators (Figs. 5(a)–5(d)) and electromagnetic induction devices (Figs. 5(e)–5(h)). Here, resonant generators usually operate at a relatively low frequency and have a property of low power densities. Resonant generators using the technology of wireless power transfer (WPT) are more suitable for miniaturization, but the need to match the vibration frequency with the mechanical resonance frequency limits its further applications. In contrast, electromagnetic induction devices can harvest higher frequencies and reach greater power densities compared to resonant generators. At the same time, the magnets and coils are too bulky, limiting their miniaturization integration.

For resonators and WPT, there have been many related types of research, and the goal is to further improve the performance of the devices. As shown in Fig. 5(a), the researchers designed an electrically small resonator composed of complementary split-ring resonators that can efficiently harvest the energy of incident electromagnetic waves to power resistive loads [56]. In the application, the resonator combined with a rectenna enables WPT and electromagnetic energy harvesting. Among them, the rectenna receives electromagnetic energy and converts it into alternating current (AC), which is then converted into DC through a rectifier circuit. This device is electrically small, making it ideal for forming arrays to harvest more energy. To overcome the collection efficiency problem, a study has proposed an energy harvester using metasurface technology [57]. The harvester consists of a set of symmetrical electric- field-coupled inductor-capacitor (ELC) resonators arranged in a 9 × 9 array, as shown in Fig. 5(b). By supplying power to the load to simulate the actual application, the experiment shows that the electromagnetic wave energy harvested by the device has almost uniform efficiency. Finally, the device achieves a harvesting efficiency greater than 92%. The insensitivity to polarization means that it has more application scenarios and can fully harvest the energy of electromagnetic waves. In Ref. [58], researchers served the human body as a low-frequency antenna to harvest electromagnetic wave energy (Fig. 5(c)). Human tissue is a material with a high dielectric constant, and the short wavelength is conducive to mutual coupling with low-frequency electromagnetic waves. Because the electrode of the device uses a low-profile, small-sized metal plate that only needs to be in contact with the human body, and has low resistance at low frequencies, the electrode is easy to integrate into mobile devices. This method can harvest more power than previous methods. For energy harvesting, electrical signals are received by electrodes in contact with the human body and then converted into electrical energy through a rectifier circuit. Therefore, the device verifies the feasibility of applying to mobile devices without antennas. Due to the narrow bandwidth of the harvesting energy resonator, a wideband ground-backed complementary split-ring resonator (WG-CSRR) array device is proposed [59]. By setting the chaotic bow-tie cavity to control the distribution of the electromagnetic field, a resonator with tunable bandwidth is formed. As shown in Fig. 5(d), the four cylinders that make up the chaotic bow-tie cavity have multiple parameters that directly determine the inductance and capacitance values of the resonator. Results show that the device achieves a half-power bandwidth of 44% at its resonant frequency, significantly increasing the resonator's bandwidth and solving the narrow-band problem.

For electromagnetic induction devices, it needs to harvest the energy of straight-line motions (e.g. walking, running), rotational motions (e.g., arm swing, leg swing), and more complex motions. In Ref. [60], researchers designed a rotating vibration energy harvesting device. Based on inertia, the device can efficiently harvest vibrational energy at ultra-low frequency (0.02 Hz). As shown in Fig. 5(e), the device is mainly composed of three parts, namely the twist-driving system, the pawl ratchet clutch system, and the magnetic coil transduction system. Among them, the twist-driving system converts linear vibrations into the rotation of the disc. The pawl-ratchet

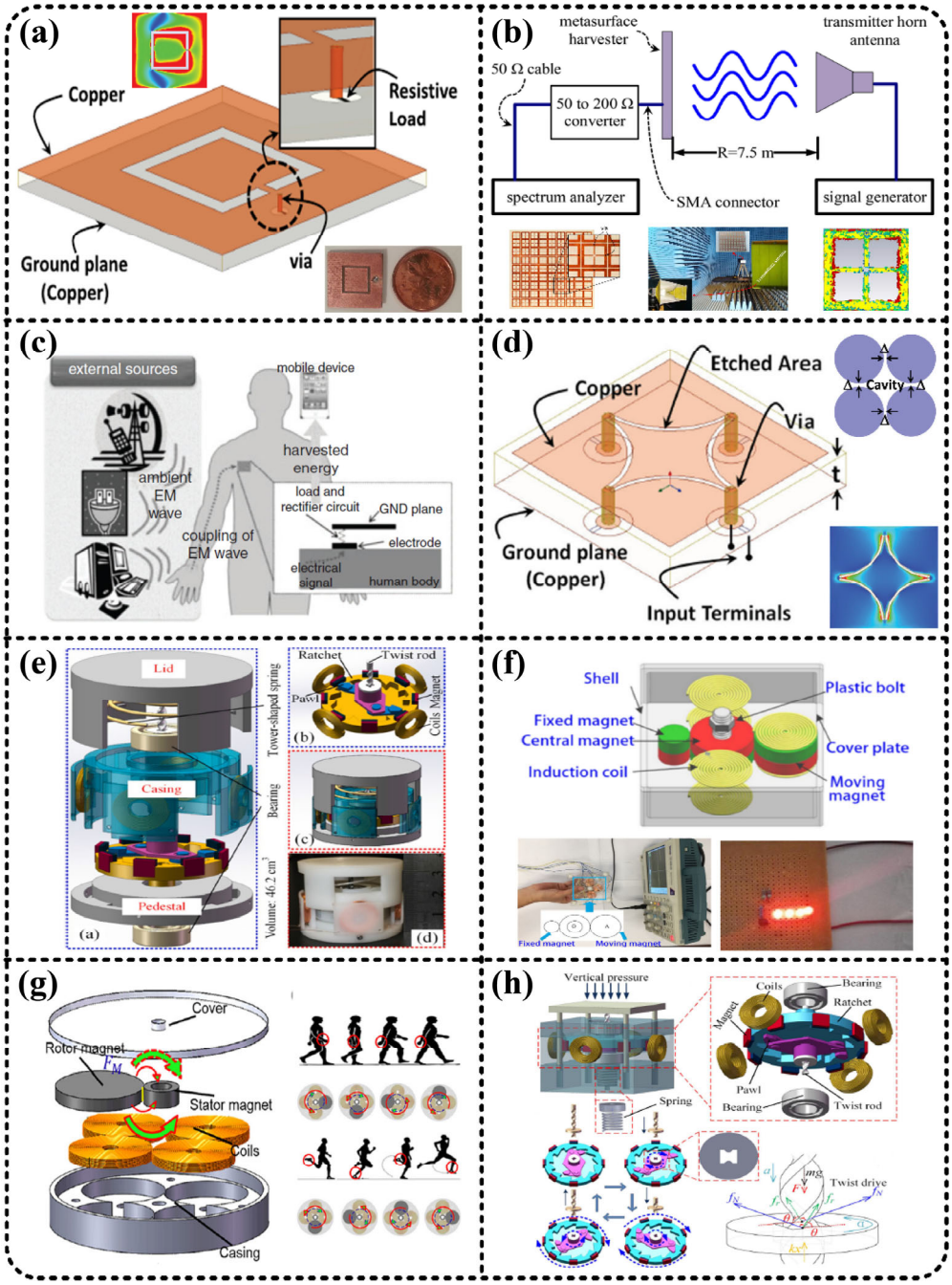

Fig. 5 Electromagnetic devices used for biomechanical energy harvesting. (a–d) Resonant generators and wireless power transfer (WPT). (a) Complementary split-ring resonators used for electromagnetic energy harvesting [56]. Reproduced with permission from Ref. [56], © AIP, 2014. (b) An energy harvester based on electric-field-coupled inductor-capacitor (ELC) resonators using metasurface technology [57]. Reproduced with permission from Ref. [57], © IET, 2018. (c) Energy harvesting using human body as antenna [58]. Reproduced with permission from Ref. [58], © IET, 2013. (d) A wideband ground-backed complementary split-ring resonator (WG-CSRR) array device with chaotic bow-tie cavity structure [59]. Reproduced with permission from Ref. [59], © AIP, 2015. (e–h) Electromagnetic induction devices with cutting magnetic flux density lines. (e) An inertial rotary energy harvester for vibrations at ultra-low frequency with high energy conversion efficiency [60]. Reproduced with permission from Ref. [60], © Elsevier, 2020. (f) A non-resonant rotational electromagnetic harvester with alternating magnet sequence [61]. Reproduced with permission from Ref. [61], © Elsevier, 2021. (g) A rotational electromagnetic energy harvester (REH) for harvesting low-frequency and irregular human motion [62]. Reproduced with permission from Ref. [62], © AIP, 2018. (h) A compact rotational electromagnetic energy harvester based on an inertial system [63]. Reproduced with permission from Ref. [63], © AIP, 2020.

clutch system transmits and stores kinetic energy, but also needs to maintain inertia in the process. The magnetic coil transducer system directly converts kinetic energy into electrical energy. The device achieves a high power of 6 mW at 0.1 Hz compressions and achieves a single-compression energy conversion efficiency of up to 97.2%. Finally, the researchers demonstrated wearable applications, such as being mounted on the soles of shoes to harvest energy from human motion, showing promising applications. In Ref. [61], researchers proposed a portable non-resonant rotating electromagnetic energy harvester. The novelty of this study is that the researchers established a Lagrangian equation for the device, and used Matlab/Simulink to analyze the output performance under different excitation frequencies. The device utilizes magnetic springs to harvest kinetic energy from low-frequency human motion and can respond to different vibrational excitations as shown in Fig. 5(f). Experiments show that the output voltage and power density of the electromagnetic energy harvester are 2.2 V and 0.024 W·mm^{-3}, respectively, when the external excitation frequency is 6 Hz. The device can light up four LEDs, which verifies the feasibility of the magnetic reed-based electromagnetic energy device to harvest low-frequency vibration energy. The device is small and bounded, the theoretical analysis is valid, and it has potential applications in self-powered portable electronics. Moreover, some researchers proposed a rotational electromagnetic energy harvester (REH) for harvesting low-frequency and irregular human motion [62]. The device consists of a cylindrical stator and a disk-shaped rotor that rotates around the stator by magnetic attraction (Fig. 5(g)) without the need for a complicated mechanism. Four wound coils are arranged in a circle around the stator. The stator is centered, reducing unnecessary friction and improving conversion efficiency. At 8 Hz, the coil can deliver a maximum power of 10.4 mW into a 100 Ω load resistance. In addition, researchers have produced a compact rotational electromagnetic energy harvester based on an inertial system [63]. Through the transmission mechanism, straight-line motion can be converted into rotary motion. As shown in Fig. 5(h), the inertial system is mainly composed of a twist driving structure and ratchet clutch structure. When the twist rod is compressed by the footsteps, the ratchet can maintain inertial rotation for 20 s, which can greatly improve the conversion efficiency of mechanical energy and promote the output of high power. The measurement shows that the peak power and the root mean square power of the device reach 32.2 and 7.7 mW, respectively. When a human footstep presses at 1 Hz, the energy harvested by the device can power an electronic hygrothermograph and 70 light-emitting diodes (LEDs).

2.3 Electrostatic energy harvesting

In general, electrostatic energy harvesting is mainly based on two fundamental phenomena, i.e., the electrostatic induction effect and the triboelectric effect. The electrostatic induction effect refers to the phenomenon that an object induces a charge and redistributes it due to the influence of other charges. And the triboelectric effect (i.e., contact electrification) describes the phenomenon that the materials become electrically charged after they are firstly in contact and then separated from others. The electric charges are induced and move under the action of external mechanical motion, and finally form a current, which means the conversion of mechanical energy to electrical energy.

2.3.1 Principles of Electrostatic Theory

Figure 6 presents electrostatic schematic diagrams and theories (see Note 3 in the ESM for the electrostatic theories in details) to explain more details about the mechanisms. For electrostatic biomechanical energy harvesting devices, the theory of electrostatic energy harvesting is mainly divided into two forms: electret [64] and triboelectricity [65, 66]. Both the theory of electrostatic electret and triboelectricity are based on the electrostatic effect, but there are essential differences in the principle of charge generation. The charge of the electret is produced via injection or electric polarization and is dispersed across the interior and exterior of the dielectric. While the triboelectric charge is only present on the surface of the medium. Its distribution results from the triboelectric effect. And the medium covers almost all materials, including metals, polymers, and wood, etc. In summary, the electret theory focuses on the creation and properties of quasi-permanent electric charges in

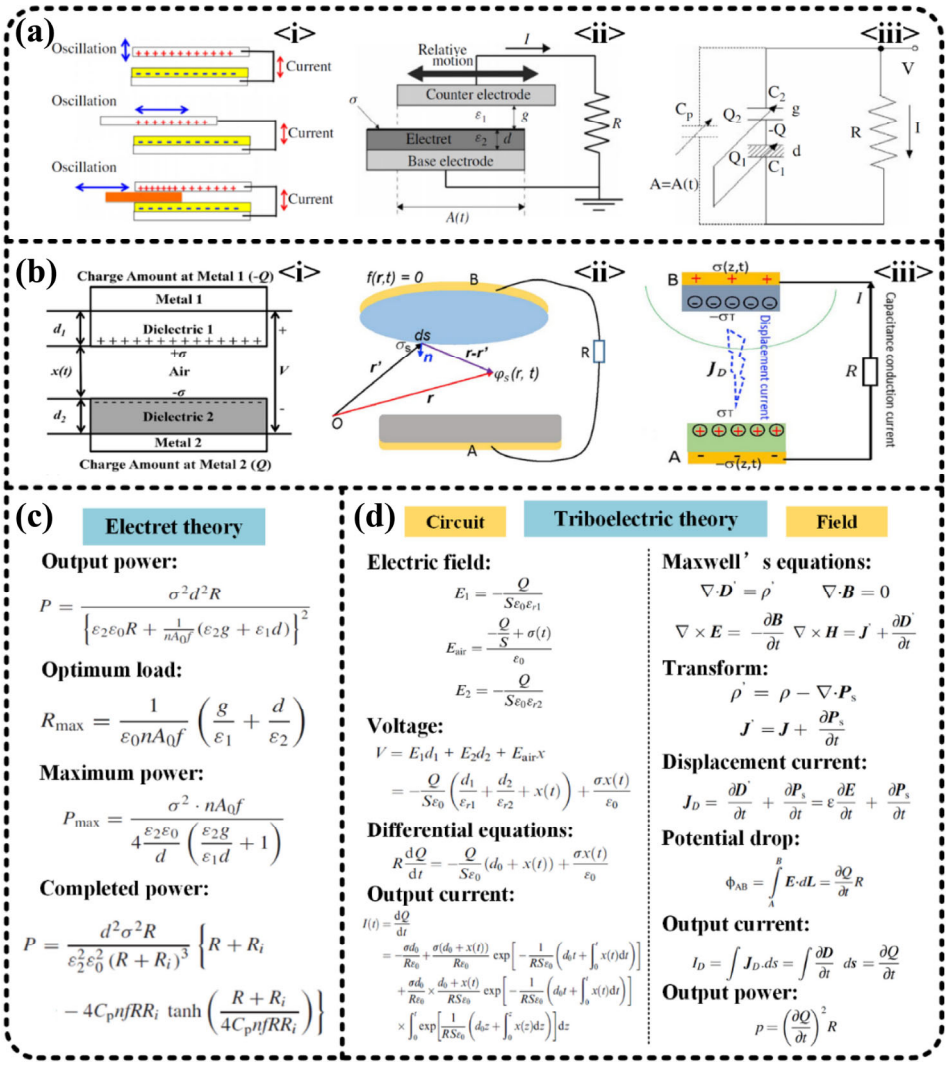

Fig. 6 Electrostatic theories for biomechanical energy harvesting. (a, b) Explanation of the electret and triboelectricity. (a) Model and diagram, including <i> principles, <ii> simplified model, and <iii> equivalent circuit of the electret generator [64]. (b) Model and diagram, including <i> dielectric-to-dielectric capacitance model [65], <ii> triboelectric nanogenerator (TENG) with an external load, and <iii> contact-separation mode TENG [66]. (c, d) Theory of the electret and triboelectricity. (c) Theory of the electret for electrostatic energy harvesting [64]. (d) Theory of triboelectricity for electrostatic energy harvesting, including circuit [65] and field model [66]. Reproduced with permission from Ref. [64], © Wiley, 2011; Reproduced with permission from Ref. [65], © the Royal Society of Chemistry, 2013; Reproduced with permission from Ref. [66], © Elsevier, 2020.

the dielectric, while the triboelectric theory deals with the temporary charge separation that occurs when two dissimilar materials are brought into contact and then separated.

The electret is a material with quasi-permanent charges [64]. Figure 6(a)<i> shows three configurations of electret generators, including closed-gap, planer oscillating, and intervening medium. Figures 6(a)<ii> and 6(a)<iii> show the simplified model and equivalent circuit of the planar oscillatory electret generator, respectively. Here, the electret and the air gap are equivalent to two capacitors in series. For electrets, the electrostatic field induces charges with opposite polarity on the electrodes, and the amount of induced charges are affected by the overlapping area between the electret and electrodes. When ignoring parasitic capacitance, the output power should be

$$P = \frac{\sigma^2 d^2 R}{\left[\varepsilon_2\varepsilon_0 R + \dfrac{1}{nA_0 f}\left(\varepsilon_2 g + \varepsilon_1 d\right)\right]^2} \tag{12}$$

where σ is the surface charge density of the electret; ε_1 and ε_2 are the relative permittivities of the air gap and the electret, respectively; d and g are the thickness of the electret and the gap distance between the electret and the electrode, respectively.

Here, if the generator has n poles with area A_0 under a rotational frequency f. Then the optimum load and maximum power are shown in Fig. 6(c), respectively. Since the power output is proportional to the square of σ, high surface charge density is effective for increasing the output of electrets.

When considering parasitic capacitance effects, a more accurate model of the output power is expressed as Eq. (13):

$$P=\frac{d^2\sigma^2R}{\varepsilon_2^2\varepsilon_0^2\left(R+R_i\right)^3}\left[R+R_i-4C_pnfRR_i\tanh\left(\frac{R+R_i}{4C_pnfRR_i}\right)\right] \tag{13}$$

For triboelectric theory, there are currently circuit models [65] and field models [66]. Triboelectric effect distinctions between materials are summarized as a list of electrical series [67], facilitating the application of the theory.

The structure of the circuit model and the calculation are simple, but there are errors. In general, the circuit model is based on capacitors as shown in Fig. 6(b)<i>, and the electric field in each region is calculated by Gauss's theorem [65]. Thus, the voltage is the product of electric field and distance (Fig. 6(d)). And then, the differential equation about the charge amount is shown as Eq. (14):

$$R\frac{\mathrm{d}Q}{\mathrm{d}t}=-\frac{Q}{S\varepsilon_0}\left[d_0+x(t)\right]+\frac{\sigma x(t)}{\varepsilon_0} \tag{14}$$

where Q, σ, and S are charges, surface charge density, and area of the electrode; ε_0, ε_{r1}, and ε_{r2} are the relative permittivities of air, dielectric 1, and dielectric 2, respectively; d_1, d_2, and x are the thickness of dielectric 1, dielectric 2, and air, respectively.

Using the initial condition, the charge solution can be expressed. Moreover, the output current can be denoted as the transfer charge amount over time. The expressions are shown in details in Fig. 6(d).

In recent years, there have been many improved theories to describe the working mechanism of triboelectricity, but none of them are universal. Until 2020, the first principle theory (i.e., field theory) of triboelectricity was proposed [66]. Since it is a field theory, it is more concerned with precision than simplicity, so it more accurately describes the behavior of triboelectricity (Figs. 6(a)<ii> and 6(a)<iii>) (see Note 4 in the ESM for the working mechanism and principle of triboelectric theories in details).

In Ref. [66], the triboelectric effect in Maxwell's equations is extracted to form an improved system of equations:

$$\begin{cases}\nabla\cdot\boldsymbol{D}'=\rho'\\ \nabla\cdot\boldsymbol{B}=0\\ \nabla\times\boldsymbol{E}=-\dfrac{\partial\boldsymbol{B}}{\partial t}\\ \nabla\times\boldsymbol{H}=\boldsymbol{J}'+\dfrac{\partial\boldsymbol{D}'}{\partial t}\end{cases} \tag{15}$$

where $\boldsymbol{D}'$, $\boldsymbol{B}$, $\boldsymbol{E}$, and $\boldsymbol{H}$ are the electric displacement, magnetic flux density, electric field, and magnetic field, respectively; ρ' and $\boldsymbol{J}'$ is the volume density of the charge and current, respectively.

Here, a transforming relationship is satisfied for the volume density of charge and current before and after the correction (Fig. 6(d)):

$$\begin{cases}\rho'=\rho-\nabla\cdot\boldsymbol{P}_s\\ \boldsymbol{J}'=\boldsymbol{J}+\dfrac{\partial\boldsymbol{P}_s}{\partial t}\end{cases} \tag{16}$$

where $\boldsymbol{P}_s$ means the existence of the charges that are independent of the presence of electric field.

Here, the potential is the key to build the equation about the charges. In circuits, the potential drop is the integral of the internal electric field along the path and is also the voltage difference formed by the passage of current across the external load resistance. Thus, the output current is shown as follows. And the solution of output voltage and power will be derived in the analytical types.

$$I_D=\int\boldsymbol{J}_D\mathrm{d}\boldsymbol{s}=\int\frac{\partial\boldsymbol{D}}{\partial t}\mathrm{d}\boldsymbol{s}=\frac{\partial Q}{\partial t} \tag{17}$$

2.3.2 *Electrostatic devices*

Electrostatic devices have been widely used in biomechanical energy harvesting and have become

an indispensable part of the wearable field due to their small size, high energy density, and high output voltage. In general, electrostatic devices can be classified into electret generators and triboelectric nanogenerators (TENGs) according to the mechanism.

For devices of electret generators, their property of quasi-permanent charges is suitable for use as wearable motion energy harvesting devices that require stability. In Ref. [68], some researchers fabricated highly efficient, flexible, and biocompatible ferroelectret nanogenerator (FENG) devices using polypropylene electret (PPFE) as the active material. There are voids and inorganic particles inside the PPFE material, which are equivalent to many electric dipoles throughout the thickness, as shown in Fig. 7(a). When pressure is applied, the change in the dipole moment causes a change in charge on the film, which in turn causes a potential difference between the electrodes of the device. In a demonstration, the energy harvested by the device lights up 20 LEDs. And then the device enables a self-powered liquid crystal display (LCD) by harvesting energy from the human touch. In addition, the research also realized a self-powered flexible, and foldable keyboard. Other researchers have proposed a linear freestanding electret generator [69]. The device uses electrodes as sliders and uses a grating structure to harvest the energy of the arm swing. Here, as shown in Fig. 7(b), the slider consists of two interdigitated electrodes on a printed circuit board (PCB). The stator consists of polytetrafluoroethylene (PTFE) electret on a polymethylmethacrylate (PMMA) substrate. The structure needs to ensure that the period of the grating and the interdigital electrodes are the same. Combined with theoretical analysis, when the effective length of the slider is half of the stator, the generator obtains the maximum power, and the output power is doubled compared with the traditional generator with the stator as the electrode. Finally, the optimized generator harvested tens of microwatts of power. In Ref. [70], some researchers have proposed hybrid structures based on electrets. The working mechanism of the device is based on charge redistribution between the two electrodes, consisting mainly of a textured support deposited with a ground electrode and the electret material. This structure (Fig. 7(c)) ensures perfect coupling between the silicone dielectric elastomer (Sylgard 186) and the electret polymer (Teflon) while improving capacitance variation and reducing von Mises stress. Among them, the flexible electrode is integrated into the elastic membrane. When the structure is deformed by force, the change in capacitance causes the charge to redistribute, which in turn causes a current to flow through the external load R. And the mechanical energy received by the device is thus converted into electrical energy. The device collected 49 μW with an electret charging to –1,000 V under a 150 MΩ load at 1 Hz and an applied strain of 50%. For electret materials, having a high charge storage capacity is a key factor in the fabrication of high-performance electret generators for wearable electronics and self-powered sensors. The work in Ref. [71] presents a new sandwich composite fluorocarbon (SCF) film, as shown in Fig. 7(d). The new material can store more residual charge than conventional electret materials (e.g., dense fluorinated ethylene propylene, fibrous polytetrafluoroethylene films). The electret generator based on this film exhibits a peak power density of ≈ 31.4 $\mu W \cdot cm^{-2}$ at a load resistance of 40 MΩ. In addition, the researchers have also applied electret generators in biomechanical energy harvesting (e.g., self-powered human breath sensors) applications.

The TENGs can be categorized into four types according to the modes, including contact-separation (CS) mode, relative-sliding (RS) mode, single-electrode (SE) mode, and freestanding (FS) mode.

Some researchers designed a 3D triboelectric nanogenerator (3D-TENG) based on the coupling of the triboelectric effect and the electrostatic induction effect [72]. As shown in Fig. 7(e), the device combines contact–separation mode and in-plane sliding mode to operate in a hybrid type. This innovative design helps to harvest random vibrational energy in multiple directions. The device is capable of harvesting an extremely wide range of ambient vibrations, achieving maximum power densities of 1.35 and 1.45 $W \cdot m^{-2}$ for out and in-plane excitation, respectively. The device can be used to harvest ambient energy in daily life and has potential applications, especially in the charging of portable electronic devices. Energy harvesting devices based on TENGs have been

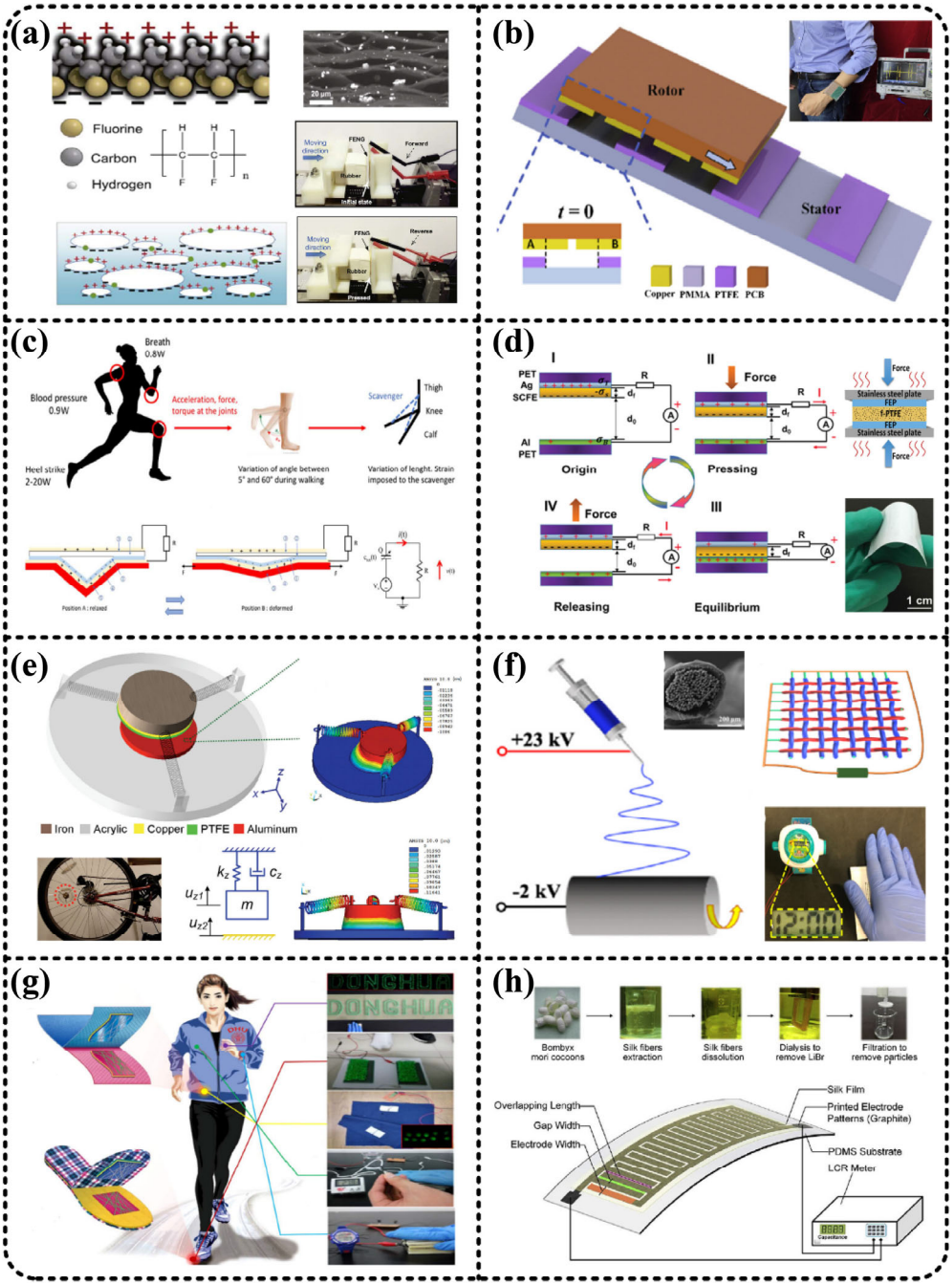

Fig. 7 Electrostatic devices used for biomechanical energy harvesting. (a–d) Electret generators devices for human motions. (a) A flexible and biocompatible polypropylene ferroelectret nanogenerator (FENG) device [68]. Reproduced with permission from Ref. [68], © Elsevier, 2016. (b) A linear freestanding electret generator with the electrodes as the slider for harvesting arm swinging energy [69]. Reproduced with permission from Ref. [69], © Elsevier, 2019. (c) An electret-based soft hybrid generator device for human body applications [70]. Reproduced with permission from Ref. [70], © IOP Science, 2019. (d) Flexible electret generator based on sandwiched composite fluorocarbon film for biomechanical energy harvesting [71]. Reproduced with permission from Ref. [71], © Wiley, 2016. (e–h) TENGs for harvesting energy. (e) 3D TENG with hybridization mode for broadband vibrational energy harvesting [72]. Reproduced with permission from Ref. [72], © Wiley, 2014. (f) Breathable, washable, and wearable woven-structured triboelectric nanogenerators utilizing electrospun nanofibers for biomechanical energy harvesting [73]. Reproduced with permission from Ref. [73], © Elsevier, 2021. (g) A wearable triboelectric nanogenerator based on a nanofibrous membrane for high-performance biomechanical energy harvesting [74]. Reproduced with permission from Ref. [74], © Elsevier, 2017. (h) Printed silk-fibroin-based triboelectric nanogenerators for multi-functional wearable applications [75]. Reproduced with permission from Ref. [75], © Elsevier, 2019.

intensively studied, however, they still face great challenges in terms of flexibility, breathability, and washability. Therefore, some researchers report a woven-structure triboelectric nanogenerator (WS-TENG) [73]. As shown in Fig. 7(f), using electrospinning, the device is fabricated from stainless steel yarns with electrospun polyamide 66 nanofibers and poly(vinylidenefluoride-co-trifluoroethylene) nanofibers. The device operates in a freestanding mode with excellent flexibility, breathability, washability, and durability. The device illuminates 58 series-connected LEDs, charges commercial capacitors, and drives portable electronics. In terms of biomechanical energy harvesting, the device is also used to detect finger movements in different states. Some researchers have fabricated a nanofibrous membrane structured triboelectric nanogenerator (NM-TENG) [74]. The device respectively provides up to 110 μA and 540 V of current and voltage output in an active area of only 16 cm^2 with a tap of the hand. Here, electrospun nanofibrous membranes are of great help in improving triboelectric polarity, mechanical strength, and surface hydrophobicity. By harvesting biomechanical energy from human motion, the device can continuously power the commercial thermal meter, electronic watch, and light with about 560 LEDs, as shown in Fig. 7(g). As a result, this device is flexible, breathable, environmentally friendly, and low-cost. With the continuous development of TENGs in the field of biomechanical energy harvesting, energy preservation and multifunctional integration are increasingly challenging. To solve the above two problems, some researchers proposed a printed silk-fibroin-based triboelectric nanogenerator (PS-TENG) [75]. The device can harvest biomechanical energy and precisely detect ambient humidity and human motions. As shown in Fig. 7(g), the study used a screen-printing process to fabricate graphite-based microscale surface patterns on polymers to form interdigitated electrodes covered with thin silk fibroin films. The device exhibits excellent performance, with output voltage, current, and power density reaching 666 V, 174.6 μA, and 412 $\mu W/cm^2$, respectively. Furthermore, the device exploited the selective absorption properties of silk fibroin to successfully distinguish the state of water molecules (i.e., liquid or gaseous) in the air. The device also integrates multiple functions such as respiration monitoring and joint motion recognition.

The output characteristics of TENG will be affected at different frequencies, which will affect its further application. At present, several works have studied and analyzed the frequency characteristics of nanogenerators for biomechanical energy harvesting [76, 77]. At low frequencies, the output of the device increases as the frequency increases. But when the frequency is too high, especially when the mechanical recovery time is longer than the external action time, the output of the device will decrease instead [78]. This is because the nanogenerators cannot return to their original position before the next force shock. Therefore, to overcome the problem of frequency influence, this part has been considered to improve the output performance of such devices by using alternative external capacitive loads [79]. This work shows that the output voltage of the device does not change with different mobile frequencies in a wide range, revealing broad prospects for biomedical applications.

2.4 Hybrid energy harvesting

At present, there are many studies on various forms of generators, but each type of generator has its own advantages and disadvantages due to different power generation mechanisms. The problem that single-type devices cannot further improve their performance (e.g., energy harvesting efficiency, energy density, and output voltage) needs to be solved urgently. Therefore, composite hybrid generators (Fig. 8), which can combine the advantages of different types of generators, have been proposed in recent years and used in biomechanical energy harvesting.

The hybrid generators that combine electromagnetic and triboelectric mechanisms are relatively easy to realize in structure, and some related studies have also been carried out. The electromagnetic-triboelectric hybrid generator fully combines the high current property of electromagnetic generators with the high voltage property of triboelectric generators, harvesting energy from two dimensions and improving efficiency.

In Ref. [80], researchers have proposed an active radio frequency identification (RFID) device for the

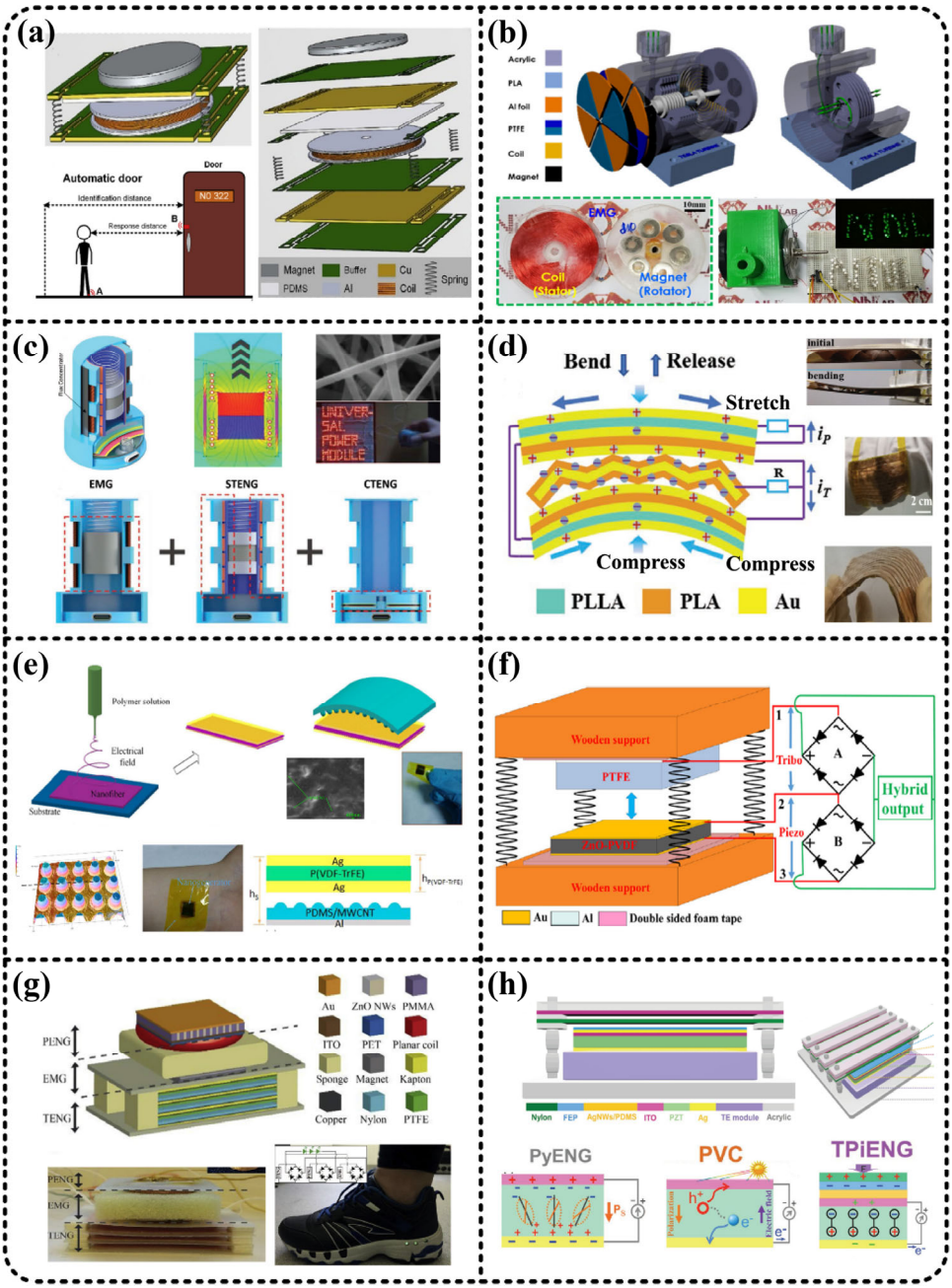

Fig. 8 Hybrid harvesting devices used for biomechanical energy harvesting. (a–c) Hybrid harvesting devices with electromagnetic and triboelectric nanogenerators. (a) A self-powered smart active RFID device integrated with a wearable hybrid nanogenerator [80]. Reproduced with permission from Ref. [80], © Elsevier, 2019. (b) A TENG/EMG hybrid nanogenerator for harvesting broadband mechanical pressure [81]. Reproduced with permission from Ref. [81], © Elsevier, 2021. (c) A universal self-chargeable power module (USPM) with a hybrid electromagnetic-triboelectric generator device [82]. Reproduced with permission from Ref. [82], © Wiley, 2020. (d–f) Hybrid harvesting devices with piezoelectric and triboelectric nanogenerators. (d) Biocompatible poly(lactic acid)-based hybrid piezoelectric and electret nanogenerator for electronic skin applications [83]. Reproduced with permission from Ref. [83], © Wiley, 2020. (e) A hybrid generator based on P(VDF-TrFE) nanofibers and PDMS/multi-walled carbon nanotube (MWCNT) composite films [84]. Reproduced with permission from Ref. [84], © Nature, 2016. (f) A flexible ZnO–PVDF/PTFE based piezo-tribo hybrid nanogenerator [85]. Reproduced with permission from Ref. [85], © Elsevier, 2018. (g, h) Hybrid harvesting devices with the multi-coupled composite generators. (g) A triboelectric-electromagnetic-piezoelectric hybrid nanogenerator [86]. Reproduced with permission from Ref. [86], © Elsevier, 2019. (h) A one-structure-based piezo-tribo-pyro-photoelectric effects coupled nanogenerator for simultaneously scavenging mechanical, thermal, and solar energies [87]. Reproduced with permission from Ref. [87], © Wiley, 2017.

Internet of Things (IoT). To overcome the problems of short communication distance and unidirectional communication of traditional passive RFID devices, a self-powered smart active RFID tag integrated with a wearable hybrid nanogenerator was proposed. Based on the triboelectric-electromagnetic hybrid mechanism, biomechanical energy can be efficiently converted into electrical energy to continuously power RFID tags. The fabricated triboelectric-electromagnetic hybrid nanogenerator (TEHN) has a maximum power density of 6.79 W/m^2. At the same time, integrating the power management module (PMM) circuit with the TEHN shortens the charging time by 50% and increases the working distance by 330% times and up to 33 m. In addition, the device can work in a duplex communication state, and successfully demonstrated the ability to remotely control an automatic door (Fig. 8(a)). Some studies have focused on hybrid energy harvesting devices consisting of triboelectric nanogenerators and rotary electromagnetic generators [81]. This device combines the two generators and is indeed capable of exporting high voltage and current. In Fig. 8(b), the TENG consists of a stator using a material of Al-covered PTFE and a patterned Al–PTFE rotator. The electromagnetic generator (EMG) consists of a coil stator and a magnet rotor. To realize a better output performance, this study integrates a Tesla turbine into the device, which guarantees the rotational condition. The researchers analyzed the dynamic balance of the rotor part of the device, so the final DC peak output voltage/current of TENG and EMG were 312.5 V/82 μA and 4.2 V/3.3 mA, respectively, while the output of the hybrid device was 332 V/3.5 mA. In addition, the device can also power LEDs by harvesting the energy of footsteps. In Ref. [82], the researchers propose a hybrid electromagnetic-triboelectric generator based on the mechanical coupling mechanism. The device is capable of high performance at very low acceleration (≤ 1 g) and low frequency (≤ 6 Hz) vibration. Here, the hybrid energy harvester consists of a combination of spring-assisted EMG, contact-separation TENG (CTENG), and interdigital electrode-based STENG (Fig. 8(c)). Due to the higher flux density of the axis of magnets, the cylindrical arrangement helps generate more flux in the coil. In the device, flux concentrators fabricated from soft magnetic materials enhance electromagnetic performance, while electrospun nanofibers enhance triboelectric performance. The device achieves a maximum DC power of 34.11 mW and performs well in harvesting biomechanical energy including walking, running, and cycling. The harvested energy successfully charges smartphones, earbuds, and smart bracelets in real time.

Another form is the hybrid generator that combines piezoelectric and triboelectric generators. In Ref. [83], the researchers combine the meso-poly(lactic acid) (meso-PLA) electret-based triboelectric nanogenerator with the double-layered poly(L-lactic acid) (PLLA)-based piezoelectric nanogenerator (PENG) for an electronic skin application (Fig. 8(d)). Here, the PENG consists of a single crystal structure, in which the double-layer PLLA film is the active layer and the PLA film is the passive layer. The structure of the cantilever leads to the output voltage and current of 70 V and 25 μA, respectively. Moreover, the output power is 0.31 mW and is 11% higher than the PENG. The hybrid device has the advantages of biocompatibility, ease of fabrication, and high output power, which is suit for biomechanical energy harvesting. In Ref. [84], a hybrid generator based on P(VDF–TrFE) nanofibers and PDMS/multi-walled carbon nanotube (MWCNT) composite films was fabricated. Among them, as shown in Fig. 8(e), P(VDF–TrFE) nanofibers were fabricated by electrospinning process and acted as a functional layer and friction layer in piezoelectric and triboelectric, respectively. The MWCNT-doped PDMS film acts as another friction layer to increase the performance of the triboelectric nanogenerator. For the triboelectric part, the output peak-to-peak voltage, power, and power density of the device are 25 V, 98.56 μW, and 1.98 mW/cm^3, respectively. For the piezoelectric part, the output peak-to-peak voltage, power, and power density were 2.5 V, 9.74 μW, and 0.689 mW/cm^3, respectively. The device is flexible, biocompatible, lightweight, and low-cost, which has obvious advantages over a single generator. In Ref. [85], the researchers set the friction layer in the structure of the triboelectric nanogenerator as a piezoelectric material, combining the two effects into one structure. As shown in Fig. 8(f), the piezo-tribo hybrid generator device is based on ZnO–PVDF films, and PTFE is

integrated through coupled fabrication techniques. It is worth noting that the ZnO-doped PVDF matrix not only has higher piezoelectric properties, but also has enhanced triboelectric properties. Measurements show that the device has an instantaneous maximum output power of about 24.5 μW/cm^2, which is about 2.5 times the output of a hybrid generator without ZnO doping. This study shows that the enhanced performance of the hybrid generator can be achieved simply by introducing ZnO nanorods into the PVDF matrix without special surface treatment or electrical polarization. Therefore, this study also provides a new method based on the simultaneous use of both effects to further improve the output of the piezoelectric triboelectric hybrid generator.

Further, some researchers have combined multiple forms of power generation to produce multi-coupled hybrid generator devices with more complex structures and more functions. In Ref. [86], some researchers firstly designed a triboelectric nanogenerator and an electromagnetic generator (EMG) in a hybrid design and then added a piezoelectric nanogenerator (PENG) to further improve the performance to form a generator with three hybrid mechanisms. To harvest human biomechanical energy, the researchers installed the device on the sole of a shoe to harvest energy from human walking. As shown in Fig. 8(g), the device has a large planar coil with a NdFeB magnet placed above the TENG. The space between the magnet and the coil is filled with a sponge, and the rebound of the sponge can separate the magnet and the coil when there is no external force. For TENG, PTFE film and Nylon film are set as top and bottom friction layers, respectively, to generate electricity by contact friction. For EMG, when the foot is pressed, the planar coil approaches the magnet, and when the force stops, the coil returns to its original position, and this way of cutting the magnetic flux density line generates an electromagnetically induced current. The PENG in this device uses ZnO nanowires, and when compressed, a potential difference is generated between the gold and ITO films due to the change of anion and cation centers in ZnO nanowires. The hybrid of the three mechanisms significantly improves the output performance of the device and enables the charging of different capacitors. Further, some researchers have proposed a multi-effect coupled nanogenerator based on a single structure, which integrates effects including thermoelectric, photoelectric, triboelectric, and piezoelectric, and can simultaneously harvest thermal, solar, and mechanical energy [87]. As shown in Fig. 8(h), by integrating pyroelectric nanogenerator (PyENG), photovoltaic cell (PVC), and triboelectric-piezoelectric nanogenerators (TPiENG) into one device and the same output electrode, the device can work whenever one energy source is available at any time. Both PyENG alone and PVC alone have higher output voltage but smaller output current compared to TPiENG alone. The device, however, combines the advantages of all single cells to generate a peak current of about 5 μA, a peak voltage of about 80 V, and a platform voltage of about 50 V. The multi-effect coupled nanogenerator of "PyENG+PVC+TPiENG" can easily charge a 10 μF capacitor to 5.1 V within 90 s. For the harvesting of biomechanical energy, the coupled multi-effect generator can also fully harvest energy and reduce waste, which has a wide range of application prospects.

In conclusion, hybrid energy harvesting technology provides a solution for sustainable energy harvesting applications [88, 89]. The system uses ambient energy such as solar, wind, wave, and thermal energy, etc., but the size scale is large, which is not suitable for harvesting energy from the human body [90, 91]. Therefore, in the future, hybrid energy harvesting technology will be combined with biomechanical wearable harvesting applications and will develop towards multi-function and miniaturization [92, 93].

3 Conclusions

In summary, the biomechanical energy harvesting for wearable electronic applications is outlined [94–97], including the working principles of various harvesting technologies [98–101, 102–104] and a summary of biomechanical energy devices [105–107]. Specifically, <i> the biomechanical energy harvesting mechanisms are reviewed, which are divided into piezoelectric effect, electromagnetic effect, and electrostatic effect; <ii> the theories of biomechanical energy harvesters are investigated, including some important formulas,

and their applicable conditions; <iii> wearable electronic devices through biomechanical energy harvesting for real-life applications are summarized; <iv> the characteristics of multi-effect coupled hybrid energy harvesting devices and the prospect of building a new generation of wearable systems are summarized.

Acknowledgements

This work is financially supported by the National Natural Science Foundation of China (Nos. 62074029, 61804023, and 61971108), the National Key R&D Program of China (No. 2022YFB3206100), the Key R&D Program of Sichuan Province (Nos. 2022JDTD0020 and 2020ZHCG0038), the Sichuan Science and Technology Program (Nos. 2020JDJQ0036, 2019YJ0198, and 2020YJ0015), and the Fundamental Research Funds for the Central Universities (No. ZYGX2019Z002).

Declaration of competing interest

The authors have no competing interests to declare that are relevant to the content of this article.

Electronic Supplementary Material: Supplementary material for the principles of piezoelectric, electromagnetic, and electrostatic theories, and the mechanism explanation of triboelectric theory is available in the online version of this article at https://doi.org/10.1007/s40544-023-0817-8.

References

[1] Bogue R. Energy harvesting: A review of recent developments. *Sens Rev* **35**(1): 1–5 (2015)

[2] Lin Z H, Cheng G, Lee S, Pradel K C, Wang Z L. Harvesting water drop energy by a sequential contact-electrification and electrostatic-induction process. *Adv Mater* **26**(27): 4690–4696 (2014)

[3] Li X W, Wu Y H, Wen D L, Chen Y, Zhang X S. Field-view theoretical model of triboelectric nanogenerators based on Laplace's equations. *Appl Phys Lett* **121**(12): 123904 (2022)

[4] Zhang X S, Han M D, Meng B, Zhang H X. High performance triboelectric nanogenerators based on large-scale mass-fabrication technologies. *Nano Energy* **11**: 304–322 (2015)

[5] Xiong J, Cui P, Chen X, Wang J, Parida K, Lin M F, Lee P S. Skin-touch-actuated textile-based triboelectric nanogenerator with black phosphorus for durable biomechanical energy harvesting. *Nat Commun* **9**: 4280 (2018)

[6] Deng H T, Zhang X R, Wang Z Y, Wen D L, Ba Y Y, Kim B, Han M D, Zhang H X, Zhang X S. Super-stretchable multi-sensing triboelectric nanogenerator based on liquid conductive composite. *Nano Energy* **83**: 105823 (2021)

[7] Hwang H J, Jung Y, Choi K, Kim D, Park J, Choi D. Comb-structured triboelectric nanogenerators for multi-directional energy scavenging from human movements. *Sci Technol Adv Mater* **20**(1): 725–732 (2019)

[8] Kwak S S, Kim H, Seung W, Kim J, Hinchet R, Kim S W. Fully stretchable textile triboelectric nanogenerator with knitted fabric structures. *ACS Nano* **11**(11): 10733−10741 (2017)

[9] Zheng Q, Zhang H, Shi B, Xue X, Liu Z, Jin Y, Ma Y, Zou Y, Wang X, An Z, Tang W, Zhang W, Yang F, Liu Y, Lang X, Xu Z, Li Z, Wang Z L. In vivo self-powered wireless cardiac monitoring via implantable triboelectric nanogenerator. *ACS Nano* **10**(7): 6510–6518 (2016)

[10] Li R, Wei X, Xu J, Chen J, Li B, Wu Z, Wang Z L. Smart wearable sensors based on triboelectric nanogenerator for personal healthcare monitoring. *Micromachines* **12**(4): 352 (2021)

[11] Meng X C, Xiao X, Jeon S, Kim D, Park B J, Kim Y J, Rubab N, Kim S M, Kim S W. An ultrasound-driven bioadhesive triboelectric nanogenerator for instant wound sealing and electrically accelerated healing in emergencies. *Adv Mater* **35**: 2209054 (2023)

[12] Zhu M, Yi Z, Yang B, Lee C. Making use of nanoenergy

from human—Nanogenerator and self-powered sensor enabled sustainable wireless IoT sensory systems. *Nano Today* **36**: 101016 (2021)

[13] Zou Y, Tan P, Shi B, Ouyang H, Jiang D, Liu Z, Li H, Yu M, Wang C, Qu X, Zhao L, Fan Y, Wang Z L, Li Z. A bionic stretchable nanogenerator for underwater sensing and energy harvesting. *Nat Commun* **10**: 2695 (2019)

[14] Cai M, Wang J, Liao W H. Self-powered smart watch and wristband enabled by embedded generator. *Appl Energy* **263**: 114682 (2020)

[15] Wang J, Jiang Z, Sun W, Xu X, Han Q, Chu F. Yoyo-ball inspired triboelectric nanogenerators for harvesting biomechanical energy. *Appl Energy* **308**: 118322 (2022)

[16] Zhang X S, Han M D, Kim B, Bao J F, Brugger J, Zhang H X. All-in-one self-powered flexible microsystems based on triboelectric nanogenerators. *Nano Energy* **47**: 410–426 (2018)

[17] Han Y, Wang W, Zou J, Li Z, Cao X, Xu S. Self-powered energy conversion and energy storage system based on triboelectric nanogenerator. *Nano Energy* **76**: 105008 (2020)

[18] Ryu H, Park H, Kim M K, Kim B, Myoung H K, Kim T Y, Yoon H J, Kwak S S, Kim J, Hwang T H, Choi E K, Kim S W. Self-rechargeable cardiac pacemaker system with triboelectric nanogenerators. *Nat Commun* **12**(1): 4374 (2021)

[19] Ji Y, Gao T, Wang Z L, Yang Y. Configuration design of $BiFeO_3$ photovoltaic devices for self-powered electronic watch. *Nano Energy* **64**: 103909 (2019)

[20] Pecunia V, Occhipinti L G, Hoye R L Z. Emerging indoor photovoltaic technologies for sustainable internet of things. *Adv Energy Mater* **11**(29): 2100698 (2021)

[21] Wen D L, Deng H T, Liu X, Li G K, Zhang X R, Zhang X S. Wearable multi-sensing double-chain thermoelectric generator. *Microsystems Nanoeng* **6**(1): 68 (2020)

[22] Noyan I D, Gadea G, Salleras M, Pacios M, Calaza C, Stranz A, Dolcet M, Morata A, Tarancon A, Fonseca L. SiGe nanowire arrays based thermoelectric microgenerator. *Nano Energy* **57**: 492–499 (2019)

[23] Ding R, Zhang X, Chen G, Wang H, Kishor R, Xiao J, Gao F, Zeng K, Chen X, Sun X W, Zheng Y. High-performance piezoelectric nanogenerators composed of formamidinium lead halide perovskite nanoparticles and poly(vinylidene fluoride). *Nano Energy* **37**: 126–135 (2017)

[24] Chen C, Bai Z, Cao Y, Dong M, Jiang K, Zhou Y, Tao Y, Gu S, Xu J, Yin X, Xu W. Enhanced piezoelectric performance of $BiCl_3$/PVDF nanofibers-based nanogenerators. *Compos Sci Technol* **192**: 108100 (2020)

[25] Lu Z, Wen Q, He X, Wen Z. A nonlinear broadband electromagnetic vibration energy harvester based on double-clamped beam. *Energies* **12**(14): 2710 (2019)

[26] Wang X X, Cao W Q, Cao M S, Yuan J. Assembling nano–microarchitecture for electromagnetic absorbers and smart devices. *Adv Mater* **32**(36): 2002112 (2020)

[27] Han M, Zhang X S, Sun X, Meng B, Liu W, Zhang H. Magnetic-assisted triboelectric nanogenerators as self-powered visualized omnidirectional tilt sensing system. *Sci Rep* **4**: 4811 (2014)

[28] Zhu G, Peng B, Chen J, Jing Q, Wang Z. L. Triboelectric nanogenerators as a new energy technology: From fundamentals, devices, to applications. *Nano Energy* **14**: 126–138 (2014)

[29] Hinchet R, Yoon H J, Ryu H, Kim M K, Choi E K, Kim D S, Kim S W. Transcutaneous ultrasound energy harvesting using capacitive triboelectric technology. *Science* **365**(6452): 491–494 (2019)

[30] Hao N, Xu Z, Nie Y, Jin C, Closson A B, Zhang M, Zhang J X J. Microfluidics-enabled rational design of ZnO micro-/nanoparticles with enhanced photocatalysis, cytotoxicity, and piezoelectric properties. *Chem Eng J* **378**: 122222 (2019)

[31] Baek C, Yun J H, Wang H S, Wang J E, Park H, Park K I, Kim D K. Enhanced output performance of a lead-free nanocomposite generator using $BaTiO_3$ nanoparticles and nanowires filler. *Appl Surf Sci* **429**: 164–170 (2017)

[32] Chopra I. Review of state of art of smart structures and integrated systems. *AIAA J* **40**(11): 2145–2187 (2002)

[33] Alavikia B, Almoneef T S, Ramahi O M. Complementary split ring resonator arrays for electromagnetic energy harvesting. *Appl Phys Lett* **107**(3): 33902 (2015)

[34] Anjum M U, Fida A, Ahmad I, Iftikhar A. A broadband electromagnetic type energy harvester for smart sensor devices in biomedical applications. *Sensors Actuators A Phys* **277**: 52–59 (2018)

[35] Pozar D M. *Microwave Engineering (Second Edition)*. New York (USA): John Wiley and Sons, 1998.

[36] Wu N, Chen S, Lin S, Li W, Xu Z, Yuan F, Huang L, Hu B, Zhou J. Theoretical study and structural optimization of a flexible piezoelectret-based pressure sensor. *J Mater Chem A* **6**(12): 5065–5070 (2018)

[37] Chen S W, Cao X, Wang N, Ma L, Zhu H R, Willander M, Jie Y, Wang Z L. An ultrathin flexible single-electrode triboelectric-nanogenerator for mechanical energy harvesting and instantaneous force sensing. *Adv Energy Mater* **7**(1): 1601255 (2017)

[38] Zhang X S, Su M, Brugger J, Kim B. Penciling a triboelectric nanogenerator on paper for autonomous power MEMS applications. *Nano Energy* **33**: 393–401 (2017)

[39] Kasap S O. *Principles of Electronic Materials and Devices (Third Edition)*. New York (USA): McGraw-Hill, 2006.

[40] Li L, Xu J, Liu J, Gao F. Recent progress on piezoelectric energy harvesting: structures and materials. *Adv Compos Hybrid Mater* **1**(3): 478–505 (2018)

[41] Khaligh A, Zeng P, Zheng C. Kinetic energy harvesting using piezoelectric and electromagnetic technologies state of the art. *IEEE Trans Ind Electron* **57**(3): 850–860 (2010)

[42] Standards Committee of the IEEE Ultrasonics, Ferroelectrics, and Frequency Control Society. IEEE Standard on Piezoelectricity. IEEE, 1988.

[43] Eltanany A M, Yoshimura T, Fujimura N, Elsayed N Z, Ebied M R, Ali M G S. Theoretical analysis of linear and nonlinear piezoelectric vibrational energy harvesters for human walking. *Jpn J Appl Phys* **54**: 10ND02 (2015)

[44] Zhang M, Gao T, Wang J, Liao J, Qiu Y, Xue H, Shi Z, Xiong Z, Chen L. Single $BaTiO_3$ nanowires-polymer fiber based nanogenerator. *Nano Energy* **11**: 510–517 (2015)

[45] Huang C T, Song J, Tsai C M, Lee W F, Lien D H, Gao Z, Hao Y, Chen L J, Wang Z L. Single-InN-nanowire nanogenerator with upto 1 V output voltage. *Adv Mater* **22**(36): 4008–4013 (2010)

[46] Park K I, Jeong C K, Ryu J, Hwang G T, Lee K J. Flexible and large-area nanocomposite generators based on lead zirconate titanate particles and carbon nanotubes. *Adv Energy Mater* **3**(12): 1539–1544 (2013)

[47] Jin C, Dong L, Xu Z, Closson A, Cabe A, Gruslova A, Jenney S, Escobedo D, Elliott J, Zhang M, Hao N, Chen Z, Feldman M D, Zhang J X J. Skin-like elastomer embedded zinc oxide nanoarrays for biomechanical energy harvesting. *Adv Mater Interfaces* **8**(10): 2100094 (2021)

[48] Manchi P, Graham S A, Patnam H, Alluri N R, Kim S J, Yu J S. $LiTaO_3$-based flexible piezoelectric nanogenerators for mechanical energy harvesting. *ACS Appl Mater Interfaces* **13**(39): 46526–46536 (2021)

[49] Guo Y, Zhang X S, Wang Y, Gong W, Zhang Q, Wang H, Brugger J. All-fiber hybrid piezoelectric-enhanced triboelectric nanogenerator for wearable gesture monitoring. *Nano Energy* **48**:152–160 (2018)

[50] Dong L, Han X, Xu Z, Closson A B, Liu Y, Wen C, Liu X, Escobar G P, Oglesby M, Feldman M, Chen Z, Zhang J X J. Flexible porous piezoelectric cantilever on a pacemaker lead for compact energy harvesting. *Adv Mater Technol* **4**(1): 1800148 (2019)

[51] Liu C, Hua B, You S, Bu C, Yu X, Yu Z, Cheng N, Cai B, Liu H, Li S, Zhang L, Wang S, Liu K, Zhang N, Liu W, Guo S, Zhao X Z. Self-amplified piezoelectric nanogenerator with enhanced output performance: The synergistic effect of micropatterned polymer film and interweaved silver nanowires. *Appl Phys Lett* **106**(16): 163901 (2015)

[52] Boylestad R L. *Introductory Circuit Analysis (Tenth Edition)*. New Jersey (USA): Prentice Hall, 2003.

[53] Griffiths D J. *Introduction to Electrodynamics (Fourth Edition)*. New Jersey (USA): Prentice Hall, 2013.

[54] Kang S H, Choi J H, Harackiewicz F J, Jung C W. Magnetic resonant three-coil WPT system between off/in-body for remote energy harvest. *IEEE Microw Wirel Components Lett* **26**(9): 741–743 (2016)

[55] Iqbal M, Nauman M M, Khan F U, Abas E, Cheok Q, Aissa B. Nonlinear multi-mode electromagnetic insole energy harvester for human-powered body monitoring sensors: Design, modeling, and characterization. *Proc Inst Mech Eng Part C J Mech Eng Sci* **235**(22): 6415–6426 (2021)

[56] Alavikia B, Almoneef T S, Ramahi O M. Electromagnetic energy harvesting using complementary split-ring resonators. *Appl Phys Lett* **104**(16): 163903 (2014)

[57] Ghaderi B, Nayyeri V, Soleimani M, Ramahi O M. Multi-polarisation electromagnetic energy harvesting with high efficiency. *IET Microwaves, Antennas Propag* **12**(15): 2271–2275 (2018)

[58] Hwang J H, Hyoung C H, Park K H, Kim Y T. Energy harvesting from ambient electromagnetic wave using human body as antenna. *Electron Lett* **49**(2): 149–151 (2013)

[59] Alavikia B, Almoneef T S, Ramahi O M. Wideband resonator arrays for electromagnetic energy harvesting and wireless power transfer. *Appl Phys Lett* **107**(24): 243902 (2015)

[60] Luo A, Zhang Y, Dai X, Wang Y, Xu W, Lu Y, Wang M, Fan K, Wang F. An inertial rotary energy harvester for vibrations at ultra-low frequency with high energy conversion efficiency. *Appl Energy* **279**:115762 (2020)

[61] Zhang J, Su Y. Design and analysis of a non-resonant rotational electromagnetic harvester with alternating magnet sequence. *J Magn Magn Mater* **540**:168393 (2021)

[62] Liu H, Hou C, Lin J, Li Y, Shi Q, Chen T, Sun L, Lee C. A non-resonant rotational electromagnetic energy harvester for low-frequency and irregular human motion. *Appl Phys Lett* **113**(20): 203901 (2018)

[63] Zhang Y, Luo A, Wang Y, Dai X, Lu Y, Wang F. Rotational electromagnetic energy harvester for human motion application at low frequency. *Appl Phys Lett* **116**(5): 53902 (2020)

[64] Suzuki Y. Recent progress in MEMS electret generator for energy harvesting. *IEEJ Trans Electr Electron Eng* **6**(2): 101–111 (2011)

[65] Niu S M, Wang S H, Lin L, Liu Y, Zhou Y S, Hu Y F, Wang Z L. Theoretical study of contact-mode triboelectric nanogenerators as an effective power source. *Energy Environ Sci* **6**(12): 3576–3583 (2013)

[66] Wang Z L. On the first principle theory of nanogenerators from Maxwell's equations. *Nano Energy* **68**: 104272 (2020)
[67] Zou H, Zhang Y, Guo L, Wang P, He X, Dai G, Zheng H, Chen C, Wang A C, Xu C, Wang Z L. Quantifying the triboelectric series. *Nat Commun* **10**: 1427 (2019)
[68] Li W, Torres D, Wang T, Wang C, Sepúlveda N. Flexible and biocompatible polypropylene ferroelectret nanogenerator (FENG): On the path toward wearable devices powered by human motion. *Nano Energy* **30**: 649–657 (2016)
[69] Wang S, Bi M, Cao Z, Ye X. Linear freestanding electret generator for harvesting swinging motion energy: Optimization and experiment. *Nano Energy* **65**: 104013 (2019)
[70] Lagomarsini C, Jean-Mistral C, Monfray S, Sylvestre A. Optimization of an electret-based soft hybrid generator for human body applications. *Smart Mater Struct* **28**(10): 104003 (2019)
[71] Wang B, Zhong J, Zhong Q, Wu N, Cheng X, Li W, Liu K, Huang L, Hu B, Zhou J. Sandwiched composite fluorocarbon film for flexible electret generator. *Adv Electron Mater* **2**(4): 1500408 (2016)
[72] Yang J, Chen J, Yang Y, Zhang H, Yang W, Bai P, Su Y, Wang Z L. Broadband vibrational energy harvesting based on a triboelectric nanogenerator. *Adv Energy Mater* **4**(6): 1301322 (2014)
[73] Guan X, Xu B, Wu M, Jing T, Yang Y, Gao Y. Breathable, washable and wearable woven-structured triboelectric nanogenerators utilizing electrospun nanofibers for biomechanical energy harvesting and self-powered sensing. *Nano Energy* **80**: 105549 (2021)
[74] Li Z, Shen J, Abdalla I, Yu J, Ding B. Nanofibrous membrane constructed wearable triboelectric nanogenerator for high performance biomechanical energy harvesting. *Nano Energy* **36**: 341–348 (2017)
[75] Wen D L, Liu X, Deng H T, Sun D H, Qian H Y, Brugger J, Zhang X S. Printed silk-fibroin-based triboelectric nanogenerators for multi-functional wearable sensing. *Nano Energy* **66**: 104123 (2019)
[76] Gai Y S, Bai Y, Cao Y, Wang E G, Xue J T, Qu X C, Liu Z, Luo D, Li Z. A gyroscope nanogenerator with frequency up-conversion effect for fitness and energy harvesting. *Small* **18**(14): 2108091 (2022)
[77] Zhang C G, He L X, Zhou L L, Yang O, Yuan W, Wei X L, Liu Y B, Lu L, Wang J, Wang Z L. Active resonance triboelectric nanogenerator for harvesting omnidirectional water-wave energy. *Joule* **5**(6): 1613–1623 (2021)
[78] Zhang X S, Han M D, Wang R X, Zhu F Y, Li Z H, Wang W, Zhang H X. Frequency-multiplication high-output triboelectric nanogenerator for sustainably powering biomedical microsystems. *Nano Lett* **13**(3): 1168–1172 (2013)
[79] Xie X K, Zhang Y, Chen C, Chen X P, Yao T, Peng M F, Chen X J, Nie B Q, Wen Z, Sun X H. Frequency-independent self-powered sensing based on capacitive impedance matching effect of triboelectric nanogenerator. *Nano Energy* **65**: 103984 (2019)
[80] Chen Y L, Liu D, Wang S, Li Y F, Zhang X S. Self-powered smart active RFID tag integrated with wearable hybrid nanogenerator. *Nano Energy* **64**: 103911 (2019)
[81] Huynh N D, Lin Z H, Choi D. Dynamic balanced hybridization of TENG and EMG via Tesla turbine for effectively harvesting broadband mechanical pressure. *Nano Energy* **85**: 105983 (2021)
[82] Maharjan P, Bhatta T, Cho H, Hui X, Park C, Yoon S, Salauddin M, Rahman M T, Rana S S, Park J Y. A fully functional universal self-chargeable power module for portable/wearable electronics and self-powered IoT applications. *Adv Energy Mater* **10**(48): 2002782 (2020)
[83] Gong S, Zhang B, Zhang J, Wang Z L, Ren K. Biocompatible poly(lactic acid)-based hybrid piezoelectric and electret nanogenerator for electronic skin applications. *Adv Funct Mater* **30**(14): 1908724 (2020)
[84] Wang X, Yang B, Liu J, Zhu Y, Yang C, He Q. A flexible triboelectric-piezoelectric hybrid nanogenerator based on P(VDF–TrFE) nanofibers and PDMS/MWCNT for wearable devices. *Sci Rep* **6**: 36409 (2016)
[85] Singh H H, Khare N. Flexible ZnO–PVDF/PTFE based piezo-tribo hybrid nanogenerator. *Nano Energy* **51**: 216–222 (2018)
[86] Rodrigues C, Gomes A, Ghosh A, Pereira A, Ventura J. Power-generating footwear based on a triboelectric-electromagnetic-piezoelectric hybrid nanogenerator. *Nano Energy* **62**: 660–666 (2019)
[87] Zhang K W, Wang S H, Yang Y. A one-structure-based piezo-tribo-pyro-photoelectric effects coupled nanogenerator for simultaneously scavenging mechanical, thermal, and solar energies. *Adv Energy Mater* **7**(6): 1601852 (2017)
[88] Ma C, Kim B, Kim S W, Park N G. Dynamic halide perovskite heterojunction generates direct current. *Energy Environ Sci* **14**(1): 374–381 (2021)
[89] Jeong C K, Kim I, Park K-I, Oh M H, Paik H, Hwang G-T, No K, Nam Y S, Lee K J. Virus-directed design of a flexible $BaTiO_3$ nanogenerator. *ACS Nano* **7**(12): 11016–11025 (2015)
[90] Huo Z Y, Lee D M, Kim Y J, Kim S W. Solar-induced hybrid energy harvesters for advanced oxidation water treatment. *iScience* **24**(7): 102808 (2021)
[91] Arroyo E, Badel A. Electromagnetic vibration energy harvesting device optimization by synchronous energy extraction. *Sensors Actuators A Phys* **171**(2): 266–273 (2011)

[92] Invernizzi F, Dulio S, Patrini M, Guizzetti G, Mustarelli P. Energy harvesting from human motion: Materials and techniques. *Chem Soc Rev* **45**(20): 5455–5473 (2016)
[93] Huo Z Y, Kim Y J, Chen Y Y, Song T Y, Yang Y, Yuan Q B, Kim S W. Hybrid energy harvesting systems for self-powered sustainable water purification by harnessing ambient energy. *Front Environ Sci Eng* **17**(10): 118 (2023)
[94] Zhang K, Wang Z L, Yang Y. Conductive fabric-based stretchable hybridized nanogenerator for scavenging biomechanical energy. *ACS Nano* **10**(4): 4728–4734 (2016)
[95] Rahman W, Ghosh S K, Middya T R, Mandal D. Highly durable piezo-electric energy harvester by a super toughened and flexible nanocomposite: Effect of laponite nano-clay in poly(vinylidene fluoride). *Mater Res Express* **4**(9): 95305 (2017)
[96] Lu L, Ding W, Liu J, Yang B. Flexible PVDF based piezoelectric nanogenerators. *Nano Energy* **78**: 105251 (2020)
[97] Xie Y, Chou T M, Yang W, He M, Zhao Y, Li N, Lin Z H. Flexible thermoelectric nanogenerator based on the MoS_2/graphene nanocomposite and its application for a self-powered temperature sensor. *Semicond Sci Technol* **32**(4): 44003 (2017)
[98] Neiss S, Goldschmidtboeing F, Kroener M, Woias P. Analytical model for nonlinear piezoelectric energy harvesting devices. *Smart Mater Struct* **23**(10): 105031 (2014)
[99] Ryu H, Yoon H J, Kim S W. Hybrid energy harvesters: toward sustainable energy harvesting. *Adv Mater* **31**(34): 1802898 (2019)
[100] Cottone F, Vocca H, Gammaitoni L. Nonlinear energy harvesting. *Phys Rev Lett* **102**(8): 80601 (2009)
[101] Kim H S, Kim J H, Kim J. A review of piezoelectric energy harvesting based on vibration. *Int J Precis Eng Manuf* **12**(6): 1129–1141 (2011)
[102] Sezer N, Koç M. A comprehensive review on the state-of-the-art of piezoelectric energy harvesting. *Nano Energy* **80**: 105567 (2021)
[103] Schure A. *Resonant Circuits*. New York (USA): John F. Rider, 1957.
[104] Boylestad R L, Nashelsky L. *Electronic Devices and Circuit Theory (Eleventh Edition)*. New Jersey (USA): Pearson Education, 2013.
[105] Ba Y Y, Bao J F, Deng H T, Wang Z Y, Li X W, Gong T, Huang W, Zhang X S. Single-layer triboelectric nanogenerators based on ion-doped natural nanofibrils. *ACS Appl Mater Interfaces* **12**(38): 42859–42867 (2020)
[106] Yang W, Chen J, Zhu G, Yang J, Bai P, Su Y, Jing Q, Cao X, Wang Z L. Harvesting energy from the natural vibration of human walking. *ACS Nano* **7**(12): 11317–11324 (2013)
[107] Zhang Y, Bao J F, Zhou X, Wu Z H, Bao F H, Zhang X S. A 10 MHz thin-film piezoelectric-on-silicon MEMS resonator with T-shaped tethers for *Q* enhancement. *Jpn J Appl Phys* **59**(1): 14002 (2020)

Xiaowen LI. She received her B.S. degree in 2020 from University of Electronic Science and Technology of China (UESTC), China. Now she is studying for a M.S. degree at UESTC, China. Her research topics focus on the micro/nano fabrication, energy harvesting, wearable electronic devices, and flexible sensors.

Xiaosheng ZHANG. He received the Ph.D. degree from Peking University in 2014. And then he joined École Polytechnique Fédérale de Lausanne (EPFL), Switzerland, as a research scientist, and also served as a research associate at The University of Tokyo, Japan. Now he is currently a professor at UESTC. In 2017, he was awarded with the Hundred-Talent Professorship by the UESTC. His research field covers the micro/nano electronic science and technology, and especially its application for self-powered multi-sensing electronics.